

Microscopic quantities in discharge in air obtained from an electro-mechanical experiment

G. Cavalleri^{1,a}, E. Cesaroni¹, E. Tonni¹, and G. Spavieri^{2,b}

¹ CNR/INFM and Dipartimento di Matematica e Fisica, Università Cattolica del Sacro Cuore, via Musei 41, 25121 Brescia, Italy

² Centro de Física Fundamental, Universidad de Los Andes, Mérida 5101, Venezuela

Received 19 September 2006 / Received in final form 20 January 2007

Published online 23 March 2007 – © EDP Sciences, Società Italiana di Fisica, Springer-Verlag 2007

Abstract. The results of an experiment of impulsive electrodynamics [Eur. Phys. J. D **15**, 87 (2001)] are shown to be due to electrons and ions in run-aways. By fitting the theoretical values with the experimental data, the values of microscopic quantities, at present unknown, can be derived, thus opening a new field of research. The obtained quantities are three, namely: (i) the contribution to air ionization due to the current (mainly of run-aways) and characterized by a parameter ρ ; (ii) the product $\zeta = n_{ei}n_{ie}$ (where n_{ei} is the number of ions extracted by one electron in run-away and n_{ie} the number of electrons extracted by one run-away ion colliding on the electrodes in electrical discharges with temperatures (for non run-aways) of $\simeq 4 \times 10^4$ K); (iii) the reconstruction time constant \mathcal{T} of the high-energy tail of the distribution function, from which we can derive the concentration per unit time of electrons and ions which become run-aways. The \mathcal{T} value is useful for the theoretical explanation of the electronic noise with power spectral density inversely proportional to the frequency.

PACS. 05.60.Cd Classical transport – 05.70.-a Thermodynamics – 47.45.-n Rarefied gas dynamics – 51.10.+y Kinetic and transport theory of gases

1 Introduction

Recently, Graneau et al. [1] have performed an interesting experiment of electrodynamics sketched in Figure 1. A capacitor bank C was charged to a voltage φ_0 and connected, after a switch S_1 , to a circuit whose sections are denoted by 1, 2, 3, 4, 5. Section 1 ends upwards with a bottom gap while Section 5 ends downwards with a top gap. A mobile section, called armature in reference [1], was initially placed with air gaps between it and the bottom electrode. By closing switch S_1 the potential difference φ_0 is applied to the two gaps in series after a very short time producing a discharge and an electric current through the circuit. The result is that the mobile armature was found to have moved upwards by an easily measurable amount when the length of the bottom gap was smaller than that of the upper gap.

We refer to a previous paper [2] for the criticism of Graneau et al. [1] interpretation relevant to their own experiment. Here, we point out that, though the Graneau experiment was the initial motivation, the present microscopic calculations are meant to generate interest in extraction microscopic quantities, especially relaxation time

scale, in new generation experiments. The main idea is that the longitudinal forces that raise the mobile armature are caused by the collisions of electrons and ions in run-away, striking the bases of the armature. Since the majority of these particles are extracted with initially high transversal velocities by other electrons and ions in run-away, a large fraction of them can collide on one basis of the armature if the corresponding gap is very small. If the gap is large, many run-away electrons and ions escape laterally outside the gap, and the impulses, and consequent pressure, are smaller than those in the smaller gap. The theoretical predictions depend on 3 parameters, namely: (i) the contribution to air ionization due to the current (mainly of run-aways) and characterized by a parameter ρ ; (ii) the product $\zeta = n_{ei}n_{ie}$ (where n_{ei} is the number of ions extracted by one electron in run-away and n_{ie} the number of electrons extracted by one run-away ion colliding on the electrodes in electrical discharges with temperatures (for non run-aways) of $\simeq 4 \times 10^4$ K); (iii) the reconstruction time constant \mathcal{T} of the high-energy tail of the distribution function, from which we can derive the concentration per unit time of electrons and ions which become run-aways. It is therefore sufficient a data fitting with 3 experimental results to obtain the wanted parameters. Actually, we

^a e-mail: g.cavalleri@dmf.unicatt.it

^b e-mail: spavieri@ula.ve

have 15 data and the redundancy improves the accuracy of the derived values.

As far as we know, there are no other methods that measure the above three parameters. Modern experiments that study discharges, especially those based on laser and imaging techniques, measure atomic spectra, temperature distributions, ionizations with great accuracy, but they do not see at all the run-away electrons that are the key of our explanation. In particular, the laser techniques are completely unable to determine the time constant \mathcal{T} necessary to reconstruct the high velocity tail of the electron distribution function. The \mathcal{T} value is necessary for the explanation of the $1/f$ noise [3] and, at present, there is a single paper [4] that tries to formulate theoretically the problem, without giving the order of magnitude.

The point is that Graneau et al. [1] have performed their own experiment completely unaware of the capacity and range of it. We encourage Graneau, Phipps Jr, and Roscoe to improve their experiment that can open a new stream of atomic physics. Some manipulations and improvements of the experimental data have been done by us in this paper, which is organized as follows.

In Section 2 we accurately examine the electrical circuit of reference [1] and, resting on the most reliable quantities measured in reference [1], we correct the values of some other quantities. These corrections partially explain the strong fluctuations in the experimental results reported in reference [1].

In Section 3, we evaluate the time required to reach a rarefaction of the air at which the air can no longer be considered as a macroscopic continuum. This time turns out to be roughly $1/60$ of the period of the underdamped oscillating current. During this time interval the pressures in the two gaps are practically the same and there is no net effect for the impulsive force on the mobile armature. In this section we use the fraction f_T of ionization only due to the thermal motion at the temperature T , i.e., we set $\rho = 0$ where ρ is the first unknown parameter.

In Section 4 we consider the conditions of the air after the time at which its particulate constitution is predominant and the mean free paths of many ions and electrons become larger than the lengths of the gaps. These ions and electrons are in run-away and, colliding on the electrodes, extract other ions and electrons with large transversal velocities v_{\perp} , which become new run-aways. Because of their large v_{\perp} , a much larger fraction of them does not hit one basis of the mobile armature in the longer gap than in the shorter gap. The consequent different pressures in the two gaps is the cause of the net impulse communicated to the mobile section (or armature) of Graneau et al.'s circuit.

In Section 5 we apply the theoretical results found in Section 4 to find the net impulse communicated to the mobile armature by the run-away ions and electrons. The data fitting with the experimental values allows the derivation of the two unknown parameters. Actually, the procedure is iterative, i.e., we first find a first order value ρ_1 for ρ . Then we recalculate all the quantities already evaluated in Section 3 with zero-order approximation. With the new values we obtain a second order value ρ_2 that

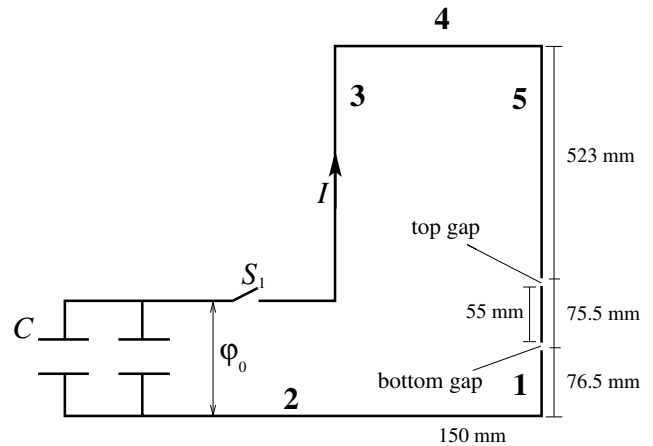


Fig. 1. Sketch of the electrical circuit used by Graneau et al. [1]. The capacitors C have been charged so as to have a potential difference φ_0 . Once closed the switch S_1 the potential difference φ_0 is applied to the two gaps in series after a very short time t_1 . Then, after another short time $t_0 - t_1$ a discharge across the two gaps make a current I flows in the circuit. The result is that the mobile section of length 55 mm receives an impulsive force toward high if the length of the bottom gap is smaller than that of the top gap.

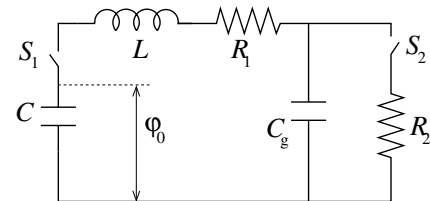


Fig. 2. Electrical scheme of the circuit used in reference [1]. A large capacitance C is initially charged with a voltage φ_0 . When the switch S_1 is closed, the voltage across the small capacitance C_g reaches the value φ_0 in a very short time t_1 . A discharge across the gap represented by C_g is equivalent to close the second switch S_2 having a resistance R in series. After the closure of S_2 we can neglect C_g and the circuit can be reduced to a series of a capacitor C , an inductor L , and a resistor $R = R_1 + R_2$.

is shown to be the final value (the iterative procedure is rapidly convergent).

We conclude in Section 6. Moreover, due to the interdisciplinary character of the physical subjects involved, we add two appendices: A — dealing with plasma and discharge electromagnetic (e.m.) waves attenuation; B — describing the behaviour of electrons and ions in run-away conditions.

2 Parameters of the electrical circuit, and time t_0 necessary to produce the initial discharge

The circuit used in reference [1] and shown in Figures 1 and 2 can be schematized by a large capacitor C , initially charged with a voltage φ_0 , followed by a switch S_1 , an

inductor L in series with a resistor R_1 , in turn in series with the two gaps synthesized by a small capacitor C_g having in parallel a switch S_2 followed by a resistor $R_2(I)$, function of the current I in the circuit. After closing switch S_1 the voltage across the two gaps rises to the value φ_0 after a very short time t_1 . Then a discharge occurs across C_g which is equivalent to the closure of switch S_2 . At this point the presence of C_g is negligible and the practical circuit is equivalent to an inductance L in series with a resistance $R = R_1 + R_2(I)$, and a capacitance C initially charged with a voltage φ_0 . The circuit is underdamped and the current, after the ignition of the discharge can be represented by a sinusoidal behaviour whose amplitude decreases exponentially. The power dissipated in the gaps if $R_1 \ll R_2(I) \simeq R$ is expressed by

$$P = RI^2 = P_0 \exp\left(-\frac{2t}{\tau}\right) \sin^2(\omega t), \quad (1)$$

where

$$\tau = 2L/R, \quad \text{and} \quad P_0 = R\varphi_0^2 C/L. \quad (2)$$

Before the ignition, the electrical resistance between the gaps is practically infinite and we have a small capacitance $C_g \simeq 10$ pF (due to the gaps and the conductors of the circuit) in series to the large capacitance $C \simeq 6$ μ F of the capacitor bank. Consequently, the voltage across the two gaps reaches the initial value φ_0 of the capacitor bank in a time

$$t_1 = \frac{\pi}{2} \sqrt{LC_g} = \frac{\pi}{2} \sqrt{LC} \sqrt{C_g/C} = 1.3 \times 10^{-3} \frac{\pi}{2\omega}, \quad (3)$$

which is roughly one thousand of a quarter of the damped current period.

The electric field \mathbf{E} is practically equal in the two gaps and accelerates the free electrons extracted from the cathode because of tunnel effect through the decreased potential barrier. Once the discharge is ignited, the current in the two gaps in series is the same. Moreover, before the formation of the run-aways described in Appendix B, the cross-sections of the ionized air gaps are the same and such are their resistivities. Consequently, the accelerated free electrons ionize other atoms and an avalanche is brought about. The space charge of any avalanche is due to a spherical ball of electrons and to a conical envelope containing the positive ions. The electric field \mathbf{E}_c due to the space charge of any avalanche on its symmetry axis is parallel to the external field \mathbf{E} outside the avalanche and antiparallel inside. As the avalanche grows, the total field $\mathbf{E} + \mathbf{E}_{ci}$ inside the avalanche decreases until it practically vanishes. Just outside the avalanche (and on its symmetry axis), $\mathbf{E} + \mathbf{E}_c \simeq 2\mathbf{E}$ and other free electrons (produced by photoionization of impurities) in the two regions around the two ends of the avalanche, are strongly accelerated and bring about other avalanches. When all the avalanches join together and reach the electrodes, a high density current (“streamer” process) begins to flow in the initial ionized channel behaving as a very thin wire connecting the electrodes. It is this very concentrated discharge that causes the ablations noted in reference [1] and also a shock wave with gas and discharge expansion.

The time t_0 taken to produce the ionized channel, and therefore to produce the initial discharge, is the sum of t_1 given by equation (3) plus the time taken by the streamer to cross the total length of the two gaps ($l = l_1 + l_2 = 20.5$ mm), i.e.,

$$t_0 = t_1 + l/v_{\text{streamer}}. \quad (4)$$

Now the propagation of the streamer is not simply limited by the drift velocity $w(E)$ where \mathbf{E} is the electric field in the gaps. First, while the avalanches are partially formed, the electric field outside them increases and, on an average, it is $2E$. Second, the propagation is mainly due to photoionization, and this implies another factor 3. Consequently, $v_{\text{streamer}} \simeq 6w(E)$. The drift velocity w is contained in equation (102) of Appendix A

$$w = \frac{eE}{m} \left\langle \frac{1}{\nu_i} - \frac{v}{3\nu_i^2} \frac{d\nu_i}{dv} \right\rangle \simeq 2 \frac{eE}{m} \left\langle \frac{1}{\nu_i} \right\rangle, \quad (5)$$

e and m being the electron charge and mass, respectively, $\nu_i = \nu_i(v)$ the electron collision frequency which is dominated by the ion interactions (as shown in Appendix A), and E the electric field that can be taken as $E \simeq \varphi_0/l$ since, as φ decreases until connecting to RI , the distances between the avalanches decrease. Using the second side of equation (111), equation (5) yields

$$w = \frac{17.9\varphi_0 \sqrt{2\pi\epsilon_0^2 (kT_{\text{streamer}})^{3/2}}}{lN_0 e^3 m^{1/2}}, \quad (6)$$

where $\epsilon_0 = 8.85 \times 10^{-12}$ Fm $^{-1}$ the vacuum permittivity, $k = 1.38 \times 10^{-23}$ JK $^{-1}$ the Boltzmann constant, and $T_{\text{streamer}} \simeq 4 \times 10^4$ K the absolute temperature of the streamer avalanches with our E values. The uncertainty is of little importance because a 100% error in w , hence in t_0 , implies a 1% error in the predictions of the height h reached by the mobile armature. The value of the initial concentration is $N_0 = 2N_a$ where $N_a = 2.7 \times 10^{25}$ m $^{-3}$ is the air concentration at sea level and at $T_a \simeq 300$ K, the factor 2 being due to the immediate dissociation of the air molecules as soon as the discharge begins. The other quantities in equation (6) takes the values: $l = 2.05 \times 10^{-2}$ m, $e = 1.6 \times 10^{-19}$ C, and $m = 9.11 \times 10^{-31}$ kg. With those value for the temperature we obtain $w \simeq 1.24 \times 10^4$ m/s, whence from equations (3) and (4) with $v_{\text{streamer}} \simeq 6w$,

$$t_0 = (8.2 \times 10^{-9} + 2.7 \times 10^{-7}) \text{ s} = 2.8 \times 10^{-7} \text{ s}, \quad (7)$$

practically independent of the C values.

3 Evaluation of the time interval during which the air in the gaps behaves as a macroscopic continuum

Denoting $p_1(t)$ and $p_2(t)$ the pressures as functions of time t in the two gaps, respectively, the net impulse on the mobile rod (or armature of mass M_A) of the circuit is given by

$$M_A v = \pi r_g^2 \int_0^\infty dt [p_1(t) - p_2(t)], \quad (8)$$

where $r_g = 2.38$ mm is the radius of the conductors (including the mobile rod) delimiting the two gaps. To obtain $p(t)$ we must also calculate the air molecule concentration $N(t)$, the air temperature $T(t)$, the velocity $V(t)$ of the air expansion, the fraction $f(t)$ of the ionized atom, the expansion velocity of the discharge channel. Fortunately, the latter quantity can be taken as equal to the velocity V of the air expansion on the front of the shock wave. Indeed, as soon as the air density decreases inside the expanding shock wave, the electron mean free paths increase and the ionization is favoured. We have therefore 5 variables, namely p , N , T , V , f and we need five equations. They are: (1) the equation for a perfect gas $p = NkT$, (2) the Boltzmann weight factor f_T plus the contribution to ionization due to the current I , (3) the Euler equation of motion for a perfect fluid, (4) the continuity equation, (5) the energy balance. Equations (1) and (2) are algebraic while (3), (4), and (5) are nonlinear differential equations.

3.1 Air as a macroscopic fluid

Let us first treat the air as a macroscopic fluid. As soon as the electrical discharge is triggered in one gap, the voltage across it decreases while it increases in the other gap, until an equal current flows in the two gaps connected in series. If in these conditions the air temperature in one gap is smaller than in the other, the ionization decreases, the electrical resistance R increases so that the power RI^2 injected in this gap increases until the two temperatures in the two gaps become equal. With the same T the two pressures p_1 and p_2 are the same so that equation (8) gives no net effect. However, when the air density $N(t)$ has dropped around a value that in the next sections we have estimated to be $N_a/86$, while the temperature T still remains very high, we must consider the particulate aspect of the air (ions and electrons) since the more energetic electrons and ions acquire mean free paths of the same order as the gap radius r_g , practically being in run-away conditions. At this level, studied in Section 4, it is $p_1(t) > p_2(t)$ if $l_1 < l_2$ where l_1 and l_2 are the lengths of gaps 1 and 2, respectively. The aim of this section is only to calculate the time interval t^* to reach the particulate aspect. Since in this first phase p , N , and T are equal in the two gaps, for simplicity we calculate t^* for a single gap of length $l = l_1 + l_2$, so as to use the total power P injected in them.

A gas at high temperature behaves as a perfect gas, so that we can use

$$p = NkT. \quad (9)$$

To the aim of calculating both the run-away current in the gaps and the energy absorbed in heating the air during the discharge, we find expressions for the average number of electrons extracted from one atom and the average energy per atom necessary to have multiple ionizations. The fraction f_{T_s} of ionized atoms in the s th level of ionization and due only to the temperature T is given by the Boltzmann weight factor. Consequently, the total number f_T of free electrons per atom (the molecules are practically all dissociated at the discharge temperature) and only due to the

thermal ionization, is given by the sum of the ionization factors

$$f_T = \sum_s \exp(-\epsilon_{is}/kT) \quad (10)$$

where ϵ_{is} is the ionization energy of the s th level per one neutral atom.

The energy required to produce the ionization per atom at temperature T is expressed by

$$\mathcal{E}_i = \sum_{s=1}^7 \epsilon_{is} \exp(-\epsilon_{is}/kT). \quad (11)$$

However, even at the discharge temperatures the second, third, etc. ionizations per atom are negligible, as shown by equations (120)–(122) of Appendix B. Consequently, in the following we only take $s = 1$. The ionization due to the current I makes the number f of free electrons increase until complete ionization is reached asymptotically (for $I \rightarrow \infty$). For nitrogen, complete ionization implies $f = 7$, and the very complicated process can be summarized as

$$f = f_T + (7 - f_T) \left\{ 1 - \exp \left[-\frac{1}{2} (\rho I_0)^2 \exp(-t/\tau) \right] \right\}, \quad (12)$$

where ρ is an arbitrary parameter to be determined by data fitting of the theoretical with the experimental results. We use therefore an iterative procedure, first putting $f = f_T$ in this section, in order to calculate the time t^* necessary to reach the particulate conditions (where diffusion dominates and we can have run-aways electrons). Then, in Section 4, we use equation (12) to express the height h reached by the mobile armature. The data fitting (performed in Sect. 5) with the experimental data gives a first order value ρ_1 for ρ . With ρ_1 we recalculate t^* and the other quantities of Section 3, which change in a modest way. The new data fitting with the experimental data gives a second order value ρ_2 with a small difference with respect ρ_1 . The use of ρ_2 in the expressions of Section 3 leads to a new t^* and other quantities with no appreciable difference from those derived with ρ_1 . The procedure converges very quickly and we take ρ_2 as the final value.

The classical equation of motion for perfect fluids, called Euler's equation, is

$$\mathbf{f}_m - \frac{1}{Nm_a} \nabla p = \frac{d\mathbf{V}}{dt} = \frac{\partial \mathbf{V}}{\partial t} + (\mathbf{V} \cdot \nabla) \mathbf{V}, \quad (13)$$

\mathbf{f}_m being the force per unit mass, which can be approximated, for gravity and small variations of altitude, with $-g\hat{\mathbf{e}}_z$ where g is the gravity acceleration and $\hat{\mathbf{e}}_z$ the unit vector of the vertical z axis. The electrical discharge is almost vertical and there is axial symmetry along the z axis so that $\mathbf{V} = V\hat{\mathbf{e}}_r$ and $\nabla = \hat{\mathbf{e}}_z(\partial/\partial z) + \hat{\mathbf{e}}_r(\partial/\partial r)$. Consequently, projecting equation (13) on $\hat{\mathbf{e}}_r$, we obtain

$$-\frac{1}{Nm_a} \frac{\partial p}{\partial r} = \frac{\partial V}{\partial t} + V \frac{\partial V}{\partial r}. \quad (14)$$

The flux of molecules through a cylinder of fixed radius $r < r_g$ is opposite to the derivative of the molecule number

contained in it

$$NV2\pi rl = -\frac{\partial}{\partial t}(N\pi r^2 l), \quad (15)$$

whence we derive the desired continuity equation for any fixed r value

$$V = -\frac{r}{2N} \frac{\partial N}{\partial t}. \quad (16)$$

This result is valid from the Eulerian point of view (fixed r). If we use the Lagrangian point of view, following the expanding front, the total number of particles contained in it is conserved, i.e.,

$$0 = d(N\pi r_F^2 l)/dt, \quad (17)$$

or

$$N = N_0 (r_0/r_F)^2 = 2N_a (r_0/r_F)^2, \quad (18)$$

where r_0 is the initial radius of the columnar discharge, r_F the radius of the expanding front, and $N_0 = 2N_a$ since practically all the diatomic molecules (of O_2 and N_2) are dissociated inside the discharge, so that as soon as the discharge is ignited, the initial monoatomic molecule concentration is twice the air molecule concentration N_a at room temperature. The advantage of the Lagrangian point of view is to reduce the differential equation (16) to the algebraic equation (18).

3.1.1 Energy balance

As said after equation (12), in this section we consider the ionization as due only to the temperature of the air (i.e., neglecting the contribution of the electric current), which implies only some percents of ionization in the first level, as shown in Appendix B. We take for the ϵ_{i1} of the first level an average, weighted value of those of nitrogen and oxygen, which turns out to be $\epsilon_{i1} = 16.06$ eV = 2.25×10^{-18} J. Using equation (11) with only $s = 1$ [see what said just after Eq. (11)] and neglecting the room temperature (compared to the very high discharge temperature), the energy balance applied to a cylinder of radius $r < r_g$ is

$$P = A\sigma_S T^4 (2\pi rl + \pi r^2) + \frac{d}{dt} [N\pi r^2 l (c_m m_a T + \epsilon_{i1} \exp(-\epsilon_{i1}/kT))], \quad (19)$$

where $l = l_1 + l_2 = 20.5$ mm is the total length of the two gaps, P the injected power. The first term inside the round brackets in the r.h.s. of equation (19) represents the radiated power through the lateral surface of the discharge column, $\sigma_S = 5.67 \times 10^{-8}$ W/(m²K⁴) being the Stefan-Boltzmann constant, A the emission coefficient of the air. The latter does not depend on the air concentration N and the absolute temperature T since, as shown in Appendix A, the attenuation distance of e.m. waves in the discharge is very small. The second term inside the round brackets in the r.h.s. of equation (19) represents the radiated power through the two bases, having assumed a

reflection coefficient 0.5. The first term inside the square brackets represents the time derivative of the thermal energy stored inside the discharge, $c_m \simeq 357$ J (kg K)⁻¹ being the specific heat per unit mass of dissociated air at constant volume [5], and $m_a = 14.4$ (in atomic unit 1.66×10^{-27} kg) the average atomic mass of dissociated air. The second term inside the square bracket denotes the time derivative of the ionization (plus excitation and molecule dissociation) energy of the air neutral atoms.

At the beginning, P is not given by equation (1) since, when the current is practically zero, all the voltage is applied to the gap. However, as soon as the discharge begins, the current is dominated by the inductance, the resistance R is variable and very high at the beginning of the discharge. But the voltage across the two gaps, expressed by $\varphi = R(I)I$, is far from being proportional to the current. The voltage, as said just before equation (3), rises to the maximum value φ_0 after the very short time t_1 and then decreases as $R(I)$ decreases with the increase of the current I . A good approximation consists in taking an exponential relaxation of φ until reaching the value RI for a time t less than an eighth of a period, i.e., for $t < \pi/(4\omega)$. Then, after such time, we take an effective value gradually decreasing with the time constant 2τ starting from the value $RI_{\text{eff}} = RI_0/\sqrt{2}$ which is $R\varphi_0(C/2L)^{1/2}$. We therefore obtain

$$\varphi = \left[\varphi_0 \exp\left(-\frac{2.1t}{t_0}\right) + RI_0 \sin \omega t \right] \Theta\left(\frac{\pi}{4} - \omega t\right) + \frac{RI_0}{\sqrt{2}} \exp\left(-\frac{t}{2\tau}\right) \Theta\left(\omega t - \frac{\pi}{4}\right), \quad (20)$$

where $\Theta(x) = 1$ for $x \geq 0$ and $\Theta(x) = 0$ for $x < 0$, while t_0 is given by equation (4).

We make the same separation for the current, i.e.,

$$I = I_0 \sin(\omega t) \Theta\left(\frac{\pi}{4} - \omega t\right) + \frac{I_0}{\sqrt{2}} \exp\left(-\frac{t}{2\tau}\right) \Theta\left(\omega t - \frac{\pi}{4}\right), \quad (21)$$

with $I_0 = \varphi_0 \sqrt{C/L}$.

Using equations (20) and (21), the expression of the power injected into the two gaps is therefore

$$P(t) = \varphi I = \varphi_0^2 \frac{C}{L} \sin \omega t \left[\exp\left(-\frac{2.1t}{t_0}\right) + \frac{RI_0}{\varphi_0} \sin \omega t \right] \times \Theta\left(\frac{\pi}{4} - \omega t\right) + \frac{1}{2} R \varphi_0^2 \frac{C}{L} \exp\left(-\frac{t}{\tau}\right) \Theta\left(\omega t - \frac{\pi}{4}\right), \quad (22)$$

where, as in equation (20), we have approximated $\exp(-2.1t/\tau) \simeq 1$ for $\omega t < \pi/4$ since $\tau \simeq 24\pi/(4\omega)$. We see in the following that equation (22) is useful for the solution of equation (19). Actually, during this phase of the discharge there is a very rapid variation of T and of the number f of extracted electrons, while the number of molecules $\mathcal{N} = N\pi r^2 l$ does not change as expressed by equation (17). Consequently, the third and fourth terms at the r.h.s. of equation (19) are dominant. We can therefore use an iterative method, neglecting in first approximation the first two terms at the r.h.s. of equation (19) in the

first stage of the discharge, i.e., from $t = 0$ to $t = t_0$. Integrating equation (19) with the use of equation (22) we obtain

$$\begin{aligned} \int_0^{t_0} P dt &= \frac{\varphi_0^2 t_0}{4.41 + \omega^2 t_0^2} \sqrt{\frac{C}{L}} [\omega t_0 - 2.1 \exp(-2.1) \sin(\omega t_0) \\ &\quad - \exp(-2.1) \omega t_0 \cos(\omega t_0)] \\ &\quad + \frac{\varphi_0^2 RC}{2L\omega} [\omega t_0 - \sin(\omega t_0) \cos(\omega t_0)] \\ &= N\pi r_0^2 l [c_m m_a T + \epsilon_{i1} \exp(-\epsilon_{i1}/kT)], \end{aligned} \quad (23)$$

where t_0 is given by equation (7) and $N = 2N_a = 5.4 \times 10^{25} \text{ m}^{-3}$.

In the second phase of the discharge, characterized by the expansion, equation (22) leads to a slow decrease of the temperature and the number \mathcal{N} of air molecules still remains constant because of equation (17) until the discharge front r_F remains smaller than the gap radius r_g . We can therefore neglect the two terms under differentiation of equation (19), take $r = r_F$ so that equation (19) reduces to

$$P = A\sigma_s T^4 (2\pi r_F l + \pi r_F^2). \quad (24)$$

At the beginning of the expansion it is $r_F = r_0$ and we derive from equation (24)

$$r_0 = l \left[\left(1 + \frac{P(t_0)}{\pi A l^2 \sigma_s T^4} \right)^{1/2} - 1 \right]. \quad (25)$$

The system of equations (23) and (25) gives r_0 and $T(r_0)$ in first approximation. Substituting equation (25) into equation (23) with $N(r_0) = 2N_a$ we obtain a transcendental equation in T only. Introducing the numerical values $l = 2.05 \times 10^{-2} \text{ m}$, $r_g = 2.38 \times 10^{-3} \text{ m}$, $N_a = 2.7 \times 10^{25} \text{ m}^{-3}$, $m = 9.11 \times 10^{-31} \text{ kg}$, $e = 1.6 \times 10^{-19} \text{ C}$, $\epsilon_0 = 8.85 \times 10^{-12} \text{ Fm}^{-1}$, $m_a = 14.4 \times 1.66 \times 10^{-27} \text{ kg} = 2.39 \times 10^{-26} \text{ kg}$, $c_m = 357 \text{ Jkg}^{-1}\text{K}^{-1}$, $A \simeq 0.4$ (for ionized air, as evaluated in Appendix A), $k = 1.38 \times 10^{-23} \text{ JK}^{-1}$, $\sigma_s = 5.67 \times 10^{-8} \text{ Wm}^{-2}\text{K}^{-4}$, $\epsilon_{i1} = 2.25 \times 10^{-18} \text{ J}$ (equivalent first ionization energy for air: see Appendix B), $P(t_0)$ given by the first term of equation (22) for $C = 6.68 \mu\text{F}$, we obtain numerically, for the case $l_1 = 1 \text{ mm}$,

$$T(r_0) = T_0 \simeq 4.24 \times 10^4 \text{ K}. \quad (26)$$

With this value, we derive from equation (25)

$$r_0 \simeq 2.14 \times 10^{-3} \text{ m} = 2.14 \text{ mm}. \quad (27)$$

At this point we calculate the energy radiated in the first stage, supposing $T = Qt$ and keeping the first order values for t_0 and r_0 . We obtain

$$\int_0^{t_0} A\sigma_s (2\pi r_0 l + \pi r_0^2) (Qt)^4 dt = A\sigma_s (2\pi r_0 l + \pi r_0^2) \frac{T_0^4}{5} t_0, \quad (28)$$

to be subtracted from the l.h.s. of equation (23). With the new net injected energy, and keeping the same t_0 values

for minimum, intermediate, and maximum values of the capacitances used by Graneau et al. [1], we obtain

$$C = 3.34 \mu\text{F}: \quad T_0 \simeq 4.44 \times 10^4 \text{ K}; \quad r_0 \simeq 1.88 \text{ mm}, \quad (29)$$

$$C = 6.68 \mu\text{F}: \quad T_0 \simeq 4.37 \times 10^4 \text{ K}; \quad r_0 \simeq 1.93 \text{ mm}, \quad (30)$$

$$C = 10.02 \mu\text{F}: \quad T_0 \simeq 4.37 \times 10^4 \text{ K}; \quad r_0 \simeq 1.95 \text{ mm}. \quad (31)$$

We see that the differences between the extreme cases (maximum and minimum used capacitances) are very small. From equation (24) written for r_F, T and r_0, T_0 , respectively, we obtain

$$T = T_0 \left(\frac{2r_0 l + r_0^2}{2r_F l + r_F^2} \right)^{1/4} \left(\frac{P}{P(t_0)} \right)^{1/4}. \quad (32)$$

3.1.2 Expansion velocity

We have now T as a function of the front radius r_F and of t through $P(t)$. The connection between r_F and $t(r_F)$ can be found if we obtain the velocity V of expansion as a function of r_F and $T[r_F, t(r_F)]$. Since there are no privileged points inside the discharge, N , T , and p are uniform from $r = 0$ to $r_M = r_F - \Delta$. Then, they have rapid variations in the small interval Δ , shown in Figures 3a and 3b. The only dependence of V on r_F remains to be found. This can be achieved by solving Euler equation (14). For $r < r_M$, the expansion velocity V can be taken as proportional to r . Then we take V to go linearly to zero in the small interval $r_M \leq r \leq r_F$, as shown in Figure 3c. We have therefore for $r \leq r_M$,

$$\begin{aligned} N(r) &= N(r_M) = N_M; & p(r) &= p(r_M) = p_M; \\ & & V &= rH(t), \end{aligned} \quad (33)$$

while, for $r_M \leq r \leq r_F$, it is

$$\begin{aligned} N &= \frac{1}{2}(N_a + N_M) \\ &\quad + \frac{1}{2}(N_a - N_M) \left(\frac{r - r_M}{\Delta} - \frac{t - t_F}{\Delta} V_M \right), \end{aligned} \quad (34)$$

$$V = V_M \left(1 - \frac{r - r_M}{\Delta} + \frac{t - t_F}{\Delta} V_M \right), \quad (35)$$

with the boundary condition $p(r_F) = p_a$. Integrating equation (14) over r from r_0 to r_M and using equation (33), we obtain

$$0 = \frac{dH}{dt} + H^2, \quad (36)$$

the solution of which is

$$H(t) = (H_0^{-1} + t - t_0)^{-1}. \quad (37)$$

Integrating equation (14) over r from r_M to r_F and using equations (33)–(35), we obtain

$$\begin{aligned} \frac{1}{m_a} (p_M - p_a) &= \int_{r_M}^{r_F} dr N \left(\frac{\partial V}{\partial t} + V \frac{\partial V}{\partial r} \right) \\ &= \frac{1}{12} V_M^2 (5N_a + N_M), \end{aligned} \quad (38)$$

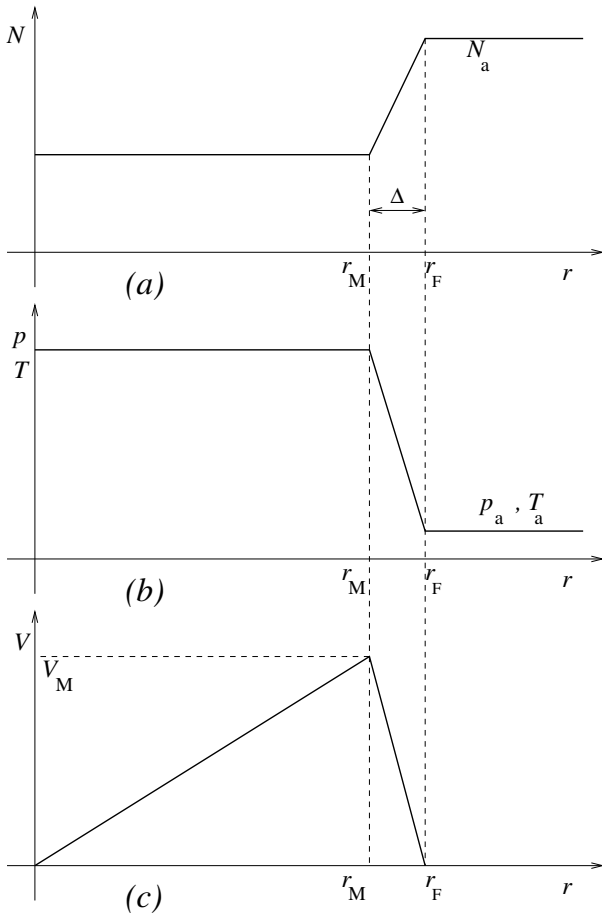


Fig. 3. Air concentration N [m^{-3}], pressures p [Nm^{-2}], temperature T [K], velocity V [ms^{-1}] vs the radius r [m] of the cylindrical expansion of the discharge at a fixed time t . The value r_F corresponds to the front of the shock wave and r_M is the preceding value at which the very rapid variations of the N , p , T , V begin. The distance $\Delta = r_F - r_M$ is very small compared to r_F and, for simplicity, we approximate the rapid variations of N , p , T , V inside Δ by straight segments. Since there are no privileged points inside r_M , it follows that N , p , T are independent of r for $r \leq r_M$, while V increases linearly with r .

which is independent of the Δ appearing in equations (34) and (35). We derive from equation (38), with the use of equations (9) and (18), where we write r_M for $r_F = r_M + \Delta$ (in practice it is $r_F \simeq r_M$ since the thickness Δ of the wave front is extremely small)

$$V_M = \left\{ \frac{12k [2T(r_0/r_M)^2 - T_a]}{m_a [5 + 2(r_0/r_M)^2]} \right\}^{1/2}, \quad (39)$$

where T is given by equation (32) and T_a is the ambient temperature.

For $r_M = r_0$, i.e., at the beginning of the expansion, it is $T_a \ll 2T$ so that equation (39) reduces to

$$V_M(r_0) \simeq \left[\frac{24kT(r_0)}{7m_a} \right]^{1/2} \simeq 1.6 \left(\frac{4kT}{3m_a} \right)^{1/2} = 1.6V_s \quad (40)$$

which is 1.6 times the speed of sound V_s at the initial temperature of the discharge. Equating equation (40) to equation (33) with the use of equation (37) for $t = t_0$, we find

$$H_0 = \frac{1}{r_0} \left[\frac{24kT(r_0)}{7m_a} \right]^{1/2}. \quad (41)$$

Finally, we derive from equations (33), (37), (39), and (41)

$$t(r_M) = t_0 - r_0 \left[\frac{7m_a}{24kT(r_0)} \right]^{1/2} + r_M \left\{ \frac{m_a [5 + 2(r_0/r_M)^2]}{12k [2T(r_0/r_M)^2 - T_a]} \right\}^{1/2}, \quad (42)$$

where T is given by equation (32) with r_M for r_F .

Since $t(r_M)$ is contained in equation (32) for T , we should solve this equation that, after eliminating the radicals, turns out to be of the 5th degree and has therefore no analytical solution. We solve it numerically setting $r_M = r_g$ so as to find the time t_g at which the expanding discharge reaches the gap boundary. We obtain

$$\begin{aligned} t_g(C = 3.34 \mu\text{F}) &\simeq 0.392 \mu\text{s} = 0.0212[2\pi/\omega(C)], \\ t_g(C = 6.68 \mu\text{F}) &\simeq 0.380 \mu\text{s} = 0.0151[2\pi/\omega(C)], \\ t_g(C = 10.02 \mu\text{F}) &\simeq 0.376 \mu\text{s} = 0.0119[2\pi/\omega(C)]. \end{aligned} \quad (43)$$

After reaching the boundaries of the gaps, the expansion goes on but the discharge is only inside the gaps. We must therefore set $r_F = r_g$ in equation (24) thus deriving from it

$$T = P(t)^{1/4} [A\sigma_s (2\pi r_g l + \pi r_g^2)]^{-1/4}. \quad (44)$$

Substituting equation (44) into equation (39) with $r_M = r_g$, we obtain $V_M(r_g, t)$. Then from the continuity equation (16) in Eulerian form and with $r = r_g$, we derive

$$N(t) = N(r_g) \exp \left[-\frac{2}{r_g} \int_{t_g}^t V(r_g, t) dt \right]. \quad (45)$$

3.2 Air as a non-macroscopic plasma of ions and electrons

If the expanding gas could be considered as a macroscopic fluid, all the found quantities would decrease with increasing r_M , hence t , until the internal pressure equates the atmospheric pressure. However, as N decreases, the air can no longer be considered as a continuous “macroscopic fluid”, but we must consider its atomic, or better ions and electrons, composition. The process becomes diffusive on the front of the expanding discharge. The pressure inside the gap does not reduce asymptotically to the atmospheric pressure p_a but, until $T \gg T_a = 300$ K, there is a diffusion from outside to inside even if $p > p_a$. The flow density from inside to outside is unidirectional and given by NV_M . Equilibrium is reached when the outflow equates the inflow which has an isotropic distribution so that only the

Table 1. Values of the concentrations N and of the temperatures T , in correspondence of the time t^* at which the regime is dominated by diffusion, for different capacitances C .

C (μF)	t^* (μs)	$N(t^*)$ (m^{-3})	$T(t^*)$ (K)
3.34	0.589	6.40×10^{23}	4.16×10^4
6.68	0.544	6.25×10^{23}	4.08×10^4
10.02	0.539	6.22×10^{23}	4.03×10^4

component against the outflow is effective. The balance is therefore

$$\begin{aligned} N(t^*)V_M(r_g) &= \int_0^{\pi/2} d\vartheta \frac{1}{2} \sin \vartheta N_a v_{300} \cos \vartheta \\ &= \frac{1}{4} N_a v_{300} = \frac{1}{4} N_a \sqrt{\frac{3k \cdot 300}{m_a}}. \end{aligned} \quad (46)$$

By means of equations (39), (45), and (46) we obtain the times t^* at which the equilibrium expressed by equation (46) is reached, and the corresponding concentrations are reported in Table 1.

A good interpolating expression for $t^*(C)$ is

$$t^*(C) = 0.674 - 0.21 (C/6.68) + 0.08 (C/6.68)^2, \quad (47)$$

where C is measured in μF and t^* in μs .

The process would become steady-state if T were constant. Actually, T decreases because the electrical current in the circuit is a damped oscillation with decay time constant τ . Consequently, $N(r < r_g)$ starts increasing until it equates the external density when $T \rightarrow 300$ K.

To formulate what said we denote by $N_{\text{in}} v_{\text{in}}$ the diffusive inflow and $N_{\text{out}} v_{\text{out}}$ the outflow. The quasi steady-state condition implies, for any $r < r_g$ value,

$$N_{\text{out}}(r) v_{\text{out}}(r) + N_{\text{in}}(r) v_{\text{in}}(r) = 0 \quad (48)$$

where, from equation (46), we have

$$4N_{\text{out}}(r_g) v_{\text{out}}(r_g) \simeq N_a v_{300}. \quad (49)$$

For simplicity we assume v_{out} to be equal to the macroscopic velocity $V(r, t_g)$ of the previous phase of ordered expansion before the diffusive quasi-equilibrium was reached. We write therefore, by means of equations (33) and (37), with $t = t_M \simeq t_g$ given by equation (43)

$$v_{\text{out}} \simeq V = \frac{r}{t_g - t_0 + 1/H_0}. \quad (50)$$

Similarly, we take, using equation (18)

$$N_{\text{out}} = 2N_a (r_0/r_g)^2 \quad (51)$$

where r_0 is given by equations (27)–(31).

The inflow, being purely diffusive, is expressed by

$$N_{\text{in}}(r) v_{\text{in}}(r) = -D \frac{d}{dr} N_{\text{in}}(r). \quad (52)$$

Denoting $\lambda(v)$ the mean free path, the diffusion coefficient is given by

$$D = \frac{1}{3} \langle \lambda(v) v \rangle, \quad (53)$$

The entering molecules of air practically do not interact with the much lighter electrons. The entering diatomic molecules of air split into two atoms but remain practically neutral. The entering neutral atoms therefore interact almost in the same way with inside neutrals and ions. It is therefore

$$\lambda(v) = \lambda = \frac{1}{\sigma_{nn} N_{\text{in}}} = \frac{1}{\pi (2R_{at})^2} \frac{1}{N_{\text{in}}}, \quad (54)$$

where $R_{at} = 6.4 \times 10^{-11}$ m is the weighted average radius of an air atom (the empirical values of the atomic radii are: 65×10^{-12} m for nitrogen and 60×10^{-12} m for oxygen, respectively [6]). Substituting equation (54) into equation (53) and calculating v at the temperature $T(r_g)$ corresponding to the end of the ordered expansion (i.e., with $r_M \simeq r_g$), we obtain

$$D = \frac{\langle v \rangle}{12\pi R_{at}^2 N_{\text{in}}} = \frac{(2kT(r_g)/m)^{1/2}}{6\pi^2 R_{at}^2} \frac{1}{N_{\text{in}}} = \frac{\bar{D}}{N_{\text{in}}}. \quad (55)$$

We derive from equations (48), (50), (52), and (55)

$$\frac{\bar{D}}{N_{\text{in}}} \frac{d}{dr} N_{\text{in}}(r) = N_{\text{out}} \frac{r}{t_g - t_0 + 1/H_0}. \quad (56)$$

Separating the variables and integrating both sides from r to r_g with $N_{\text{in}}(r_g) = N_a - N_{\text{out}}$, we obtain

$$\begin{aligned} N(r) &= N_{\text{in}}(r) + N_{\text{out}} = N_{\text{out}} + (N_a - N_{\text{out}}) \\ &\times \exp \left[N_{\text{out}} \frac{r^2 - r_g^2}{2\bar{D}(t_g - t_0 + 1/H_0)} \right], \end{aligned} \quad (57)$$

with N_{out} given by equation (51), \bar{D} by equation (55), H_0 by equation (41), t_0 by equations (29)–(31), and t_g by equation (43). The density $N(r)$ of equation (57) is the wanted expression used near the end of Appendix B.1.

4 Electrons and ions in run-away as the cause of the net impulse given to the circuit mobile section of Graneau experiment

The preceding section was useful to find the concentration $N(r)$, the temperature T , and the time $t_M \simeq t_g$ necessary to reach the quasi-equilibrium condition due to back diffusion. However, during that phase the pressures p_1 and p_2 in the two gaps of Graneau et al. experiment [1] are equal so that there is no net impulse on the mobile armature (as denoted by the authors in Ref. [1]). We outline here the mechanism that leads to a net impulse communicated to the armature.

When the quasi-equilibrium is reached, $N(r)$ is sufficiently low, while the temperature and the electric field are sufficiently high, to allow the production of run-aways, as examined in Appendix C. An electron in run-away hitting an electrode can extract an average number n_{ee} of electrons and a number n_{ei} of ions. Similarly, an ion in

run-away can extract n_{ii} ions and n_{ie} electrons. However, the ions extracted by an ion fall on the electrode after describing a short section of a parabola and are therefore not effectively contributing to the impulse transmitted to the armature. Consequently, n_{ii} does not matter. Similarly, for n_{ee} . What counts is n_{ei} and n_{ie} .

As far as we know, there are no experimental values for those two numbers in the extreme conditions of an electrical discharge. We therefore leave them as two unknowns to be determined by data fitting with the experimental results of Graneau et al. experiment [1].

The electrons and ions extracted from the electrode (because of the impinging on it of either an electron or an ion) have a distribution of velocities and the more energetic are already in run-away condition. Their trajectory is parabolic and the probability of impinging on the mobile armature is higher for the smaller gap. In the larger gap a good amount of electrons (or ions) in run-away can get out of the gap, so that they do not contribute to the impulse communicated to the armature. The successive extractions exalt the impulse differences to the armatures in the two gaps. The current in the gaps becomes mainly due to the run-aways and the avalanche process is limited by the drop of the potential across the two gaps in series.

To formulate in a quantitative way the above process that lead to a pressure difference [expressed by Eq. (18)] we proceed as follows. We first find a plausible distribution for the velocities of the extracted electrons (or ions). Then we calculate the probability that an extracted electron (or ion) can impinge on the armature. The point of extraction is generic and we have to perform an average. Finally, considering the very large number of successive extractions, we obtain a convergent geometric series that depends on the gap width (l_1 or l_2) and gives the differences on the impulses communicated to the armature in the two gaps.

The energy acquired by an electron in traversing a gap of height l_1 is eEl_1 , the electric field E being equal in the two gaps in series. An energy balance yields

$$eEl_1 = \frac{1}{2}Mu_0^2 + U_{\text{extr}} + U_{\text{lost}}, \quad (58)$$

where M and u_0 denote the mass and the speed, respectively, of an extracted ion, U_{extr} the extraction energy, and U_{lost} the energy transformed into thermal energy of the electrode. Now U_{extr} is of the order of some eV and is therefore negligible compared to $eEl_1 > 200$ eV even with the minimum used height $l_1 \simeq 1$ mm and at the end of the effective damped oscillation of the current in the circuit. U_{lost} is statistical and can range from almost zero to eEl_1 . The maximum speed is therefore

$$u_{0\text{max}} = \sqrt{2eEl_1/M} = \sqrt{2Al_1}. \quad (59)$$

A similar reasoning holds for the maximum speed $v_{0\text{max}}$ of an electron extracted by an ion. It is therefore

$$v_{0\text{max}} = \sqrt{2eEl_1/m} = \sqrt{2al_1}. \quad (60)$$

The distribution function $g_e(v_0, \theta)$ of the extracted electrons has statistically its maximum at $v_0 \simeq v_{0\text{max}}/2$, being θ the angle between the initial velocity of the extracted

electron and the outward normal to the electrode. For the θ dependence we approximate as follows. We suppose that a fraction \mathcal{F} of the initial velocities just after an extraction from an electrode be mainly along the symmetry axis of the two gaps, denoted as z , while the complement $1 - \mathcal{F}$ be mainly in the plane xy of one of the electrodes. The fraction \mathcal{F} can easily be found taking into account that the angular distribution of the extracted electrons is due to Coulomb scattering with the screening conditions studied by Brooks and Herring [7], whose differential cross-section is expressed by equation (A.15) of reference [8] which reads

$$\sigma(v, \mu_s) = C[(1 - \mu_s) + D]^{-2}, \quad (61)$$

where μ_s is the cosine of the scattering angle ϑ_s and where C and D summarize quantities independent of the cosine μ_s of the scattering angle ϑ_s . Now D is important to eliminate the divergences of the Coulomb scattering at low ϑ_s angles, i.e., for $\mu_s \rightarrow 0$. However, in our case we consider angles $\vartheta_s > \pi/2$ so that D is negligible. We therefore approximate the electrons (or ions) extracted with initial velocities having scattering angles ϑ_s (with respect to the impinging electron, or ion) between $\pi/2$ and $3\pi/4$ as all moving in the xy plane (corresponding to $\vartheta_s = \pi/2$), while those with $3\pi/4 \leq \vartheta_s < \pi$ as moving along the z -axis. Consequently, $1 - \mathcal{F}$ is proportional to the cross-section

$$\begin{aligned} 1 - \mathcal{F} &\propto \int_{\pi/2}^{3\pi/4} d\vartheta_s \sin \vartheta_s (1 - \mu_s)^{-2} \\ &= \int_{-2^{-1/2}}^0 d\mu_s (1 - \mu_s)^{-2} \\ &= [(1 - \mu_s)^{-1}]_{-2^{-1/2}}^0 = 0.4142. \end{aligned} \quad (62)$$

Similarly

$$\begin{aligned} \mathcal{F} &\propto \int_{3\pi/4}^{\pi} d\vartheta_s \sin \vartheta_s (1 - \cos \vartheta_s)^{-2} \\ &= [(1 - \mu_s)^{-1}]_{-1}^{-2^{-1/2}} = 0.0858. \end{aligned} \quad (63)$$

Since $1 - \mathcal{F} + \mathcal{F} = 1$, we find the constant of proportionality and obtain

$$1 - \mathcal{F} = 0.8284; \quad \mathcal{F} = 0.1716. \quad (64)$$

A plausible velocity distribution that accounts for multiple scatterings is sinusoidal. We can therefore take the following normalized distribution function of the horizontal velocities v_0

$$g_{xy}(v_0) = \frac{0.8284\pi}{2v_{0\text{max}}} \sin\left(\frac{\pi v_0}{v_{0\text{max}}}\right) \Theta(v_{0\text{max}} - v_0), \quad (65)$$

where $\Theta(x) = 1$ for $x > 0$ and $\Theta(x) = 0$ for $x < 0$.

Again with the use of equation (64), the distribution function for the velocities supposed along the z -axis is given by

$$g_z(v_0) = \frac{0.1716\pi}{2v_{0\text{max}}} \sin\left(\frac{\pi v_0}{v_{0\text{max}}}\right) \Theta(v_{0\text{max}} - v_0). \quad (66)$$

We first calculate the probability that the fraction of the electrons with initial velocities parallel to the plane of the electrode (lying in the xy -plane), reach the other face of the gap. For those electrons we can still neglect the stray fields due to the boundary, because the larger loss of those coming out radially is partially compensated by those pointing toward the center of the gap, while the radial stray fields have a negligible effect on the electrons having velocities roughly transversal to them. Consequently, considering $\mathbf{E} = E\hat{e}_z$, the position of an electron starting from $r\hat{e}_x$ at $t = 0$, is expressed by

$$\mathbf{R}(t) = r\hat{e}_x + v_0t(\hat{e}_x \cos \phi + \hat{e}_y \sin \phi) + \frac{e}{2m}Et^2\hat{e}_z, \quad (67)$$

and the time Δt taken to reach the armature is

$$\Delta t = (2ml_1/eE)^{1/2}. \quad (68)$$

The condition that the electron impinges on the armature (rather than leaving the region of space of the gap) is obtained imposing that the component of $\mathbf{R}(\Delta t)$ on the xy plane has an absolute value less than r_g . It is

$$[r^2 + v_0^2\Delta t^2 + 2rv_0\Delta t \cos \phi]^{1/2} \leq r_g, \quad (69)$$

whence

$$v_0 \leq v_{lc} = \left(\frac{eE}{2ml_1}\right)^{1/2} [(r_g^2 - r^2 \sin^2 \phi)^{1/2} - r \cos \phi]. \quad (70)$$

The average probability of hitting the armature is therefore given, with the use of equations (65), (156), and (157),

$$\begin{aligned} \mathcal{P}_{e_{xy}}(l, t) &= \int_0^\pi d\phi \frac{1}{\pi} \int_0^{r_g} dr r q(r) \int_{v_{0m}}^{v_{lc}(t, r, \phi)} dv_0 g_{xy}(v_0) \\ &= \frac{0.8284}{2\pi} \int_0^\pi d\phi \int_0^{r_{\max}} dr \frac{2r}{r_{\max}^2} \\ &\times \left\{ \cos\left(\frac{\pi v_{0m}}{v_{0\max}}\right) - \cos\left[\frac{\pi v_{lc}(t, r, \phi)}{v_{0\max}}\right] \right\}, \quad (71) \end{aligned}$$

where $v_{0\max}$ is given by equation (60), and $q(r)$ is the radial distribution of run-aways obtained in Appendix B.1 and given by equation (157).

A similar expression is obtained for the probability $\mathcal{P}_i(l, t)$ that an ion reaches the opposite electrode. Fortunately, the ratios of the velocities appearing in equation (71) and all the velocities turn out to be inversely proportional to the square root of the masses, so that

$$\mathcal{P}_i(l, t) = \mathcal{P}_{e_{xy}}(l, t) = \mathcal{P}_{xy}(l, t). \quad (72)$$

The dependence $v \propto m^{-1/2}$ is clear for $v_{0\max}$ and v_{lc} given by equations (60) and (70), respectively. For v_{0m} , this conclusion is shown in Appendix B.

Let us now calculate the probability \mathcal{P}_z that either an ion (or an electron) having initial velocity $\mathbf{v}_0 = v_0\hat{e}_z$ reach the other face of the gap. If there were no stray, radial fields, all the fraction \mathcal{F} [given by Eq. (64)] of these ions would reach the other face of the gap. In this case

the stray, radial field E_r cannot be neglected. Since any gap face is equipotential, $E_r(z = 0) = E_r(z = l) = 0$, and also $E_r(l/2) = 0$ because of symmetry, we can take a sinusoidal behaviour for it

$$\mathbf{E}_r(r, z, l_1) = \hat{\mathbf{r}} E_{r0}(r, l_1) \sin\left(\frac{2\pi z}{l_1}\right), \quad (73)$$

where $\hat{\mathbf{r}}$ is the radial unit vector and $E_{r0}(0) = 0$ because of symmetry. The dependence $E_{r0}(r)$ has been found exploiting the results of a previous paper [9]. Consequently, we obtain

$$\begin{aligned} E_r(r, z, l_1) &= \frac{RI_0}{l\sqrt{2}} \exp\left(-\frac{t}{2\tau}\right) \frac{1.7l_1/l}{1 + 32(l_1/l)^2 + 6.5(l_1/l)^3} \\ &\times \sin\left(\frac{\pi r/r_g}{1 + 2.6l_1/l}\right) \sin\left(\frac{2\pi z}{l_1}\right). \quad (74) \end{aligned}$$

Because of E_r , an ion undergoes a radial displacement given by

$$\Delta r = \int_0^{\Delta t} dt \int_0^t dt' \frac{e}{m} E_r(r, z, l_1), \quad (75)$$

where Δt is the time taken by the ion to traverse the gap of length l_1 . The ion impinges on opposite face of the gap if

$$\Delta r < r_g - r. \quad (76)$$

As soon as an ion comes out of the cylinder of radius r_g , it finds the atmospheric concentration and loses the largest part of its momentum against the air molecules.

In order to perform the integration (75) we must express z as a function of the dummy variable t' . This is easily obtained if we keep constant $E_z = E\hat{e}_z$ so that

$$z = v_0t' + \frac{e}{2m}Et'^2. \quad (77)$$

For simplicity, we keep $E_{r0}(r)$ equal to the value corresponding to the starting r of the ion, and we perform numerical integration of equation (75) for different l_1 , r , and v_0 (contained in Δt) values, thus obtaining, by means of interpolation,

$$\begin{aligned} \frac{v_0}{v_{0z_m}(l_1, r)} &= \left[-8.79 \times 10^{-3} + 1.069 \left(\frac{r}{r_g}\right)^2 \right] \\ &\times \left[1.105 - 0.269 \left(\frac{9 \times 10^{-3} - l_1}{l}\right) \right]. \quad (78) \end{aligned}$$

The run-away ions (or electrons) reaches the mobile armature only if $v_{0z} \geq v_{0z_m}(l, r)$. We therefore obtain for the probability \mathcal{P}_z that an ion (or an electron) hits the armature face if its starting velocity is $\mathbf{v}_0 = v_0\hat{e}_z$, also using equations (63), (64), (78), and (157),

$$\mathcal{P}_z(l, t) = \frac{0.1716}{2\pi} \int_0^{r_{\max}} dr \frac{2r}{r_{\max}^2} \left\{ \cos\left[\frac{\pi v_{0z_m}(l, r)}{v_{0\max}}\right] + 1 \right\}, \quad (79)$$

similar to equation (71) but with $v_{0\max}$ [still given by Eq. (60)] for $v_{lc}(t, r, \phi)$ and no dependence on ϕ .

If n_{ei} ions are extracted from the armature by one electron, the number of run-away ions that reach the opposite electrode is $n_{ei}(\mathcal{P}_z + \mathcal{P}_{xy})$. Then these ions extract $n_{ie}n_{ei}(\mathcal{P}_{xy} + \mathcal{P}_z)$ electrons and, of these, the fraction

$$\begin{aligned} n_{\text{run}}(l_1) &= n_{ei}n_{ie}[\mathcal{P}_z(l_1, t) + \mathcal{P}_{xy}(l_1, t)]^2 \\ &= \zeta[\mathcal{P}_z(l_1, t) + \mathcal{P}_{xy}(l_1, t)]^2 \end{aligned} \quad (80)$$

reaches the armature. The process repeats and, if the factor $n_{\text{run}} < 1$, we have a convergent geometrical series so that the total number of electrons impinging on the armature and due to an initial electron in run-away is

$$n_{\text{tot}}(l_1) = [1 - n_{\text{run}}(l_1)]^{-1}. \quad (81)$$

Because of the symmetry in the subscripts i and e of equation (80), the same series holds for ions.

The net impulse communicated to an armature by an electron impinging on it is expressed by

$$\mathcal{I} = mv = \sqrt{2meEl_1}. \quad (82)$$

However, during the transit time, there is an attraction of the considered armature by part of the electron in flight causing a force $eE/2$ (the field due to a single armature is $E/2$). This reaction force produces an impulse with opposite sign with respect to equation (82) given by

$$\mathcal{I}_{re} = -\frac{1}{2}eE\Delta t = -\frac{eE}{2}\sqrt{\frac{2l_1}{a}} = -\frac{1}{2}\mathcal{I}. \quad (83)$$

The net impulse is therefore from equations (82) and (83)

$$\mathcal{I}_{\text{net}} = \mathcal{I} + \mathcal{I}_{re} = \frac{1}{2}\mathcal{I} = \sqrt{\frac{1}{2}meEl_1}. \quad (84)$$

An initial electron produces a total number $n_{\text{tot}}(l_1)$ of run-aways given by equation (81), so that the total net impulse is expressed by

$$\mathcal{I}_{\text{tot}} = [1 - n_{\text{run}}(l_1)]^{-1}\sqrt{\frac{1}{2}meEl_1}, \quad (85)$$

where $n_{\text{run}}(l_1)$ is given by equation (80).

The net average force due to single initial electrons in run-away is given by \mathcal{I}_{net} times the frequency ν_b of the bounces on the considered armature. It is

$$\nu_b = (\Delta t_i + \Delta t_e)^{-1} = \left[\frac{2l_1}{eE}(\sqrt{m} + \sqrt{M}) \right]^{-1}, \quad (86)$$

so that the net force on the armature on which electrons (due to a single initial electron in run-away) impinge is

$$F_e^1(l_1) = \mathcal{I}_{\text{tot}}\nu_b = \frac{eE}{2[1 - n_{\text{run}}(l_1)]} \frac{\sqrt{m}}{\sqrt{m} + \sqrt{M}}. \quad (87)$$

However, the electric field value E versus time is a damped oscillation so that E inverts its direction after only half-period and then ions, instead of electrons, impinge on the

armature. Being the oscillations slowly damped, in first approximation we may take

$$F_{\text{net}}^1(l_1) = \frac{1}{2}[F_e(l_1) + F_i(l_1)] = \frac{eE}{4[1 - n_{\text{run}}(l_1)]}, \quad (88)$$

that is symmetric with respect to ions and electrons.

The total net force on the mobile armature is the difference of the forces on the two bases of the armature, i.e.,

$$\begin{aligned} F_{\text{net}}^1 &= F_{\text{net}}^1(l_1) - F_{\text{net}}^1(l_2) \\ &= \frac{eE}{4} \left[\frac{1}{1 - n_{\text{run}}(l_1)} - \frac{1}{1 - n_{\text{run}}(l_2)} \right]. \end{aligned} \quad (89)$$

If $I_{\text{run}} = dN_{\text{run}}/dt$ is the total current of run-aways, i.e. the number of electrons and ions in run-away per unit time expressed by equation (164), the total net impulse on the mobile armature is

$$\begin{aligned} \Gamma_{\text{tot}} &= \int_{t^*}^{\infty} dt I_{\text{run}} \frac{e}{4} E_0 \exp\left(-\frac{t}{2\tau}\right) \\ &\quad \times \left[\frac{1}{1 - n_{\text{run}}(l_1)} - \frac{1}{1 - n_{\text{run}}(l_2)} \right], \end{aligned} \quad (90)$$

where $t^*(C)$ is given by equation (47).

Finally, $M_A = 17$ g is the mass of the mobile armature [1], the maximum displacement or height h it would reach in absence of friction is

$$h = \Gamma_{\text{tot}}^2 (2M_A^2 g)^{-1}. \quad (91)$$

Our calculations are performed using the damped oscillations for the current in the circuit given in reference [1], which implies symmetry between ions and electrons. We suggest that other experiments of the kind of Graneau et al. but with an overdamped discharge, imply an asymmetry between $F_e^1(l_1)$ given by equation (88), and the corresponding for ions

$$F_i^1(l_1) = F_e^1(l_1)\sqrt{M/m}. \quad (92)$$

A dedicated experiment performed in this condition would be able to discriminate $F_e^1(l_1)$ and $F_i^1(l_1)$, for example, using first a strongly damped positive E , and repeating the experiment using a strongly damped negative E . The outcome of such a repetition of the Graneau et al. experiment could be used as a test of our theoretical analysis that predicts that run-aways are responsible for the force difference on the mobile armature.

5 Data fitting and the iterative procedure

As said in the Introduction, we apply our theoretical results to find the h values, i.e., the upward maximum displacements of the mobile armature for different values of the smaller gap l_1 and capacitance C . We use equation (91), where Γ_{tot} is given by equation (90), in which I_{run} is expressed by equation (164) and $n_{\text{run}}(l)$ by

Table 2. Comparison between the theoretical predictions vs. experimental data for the height h of the mobile rod.

l_1 (mm)	C (μF)	t_2^* (μs)	h_{exp} (mm)	h (mm)
1.0	3.34	0.588	3	4.2
1.0	5.01	0.561	10.3	11.8
1.0	5.01	0.561	5.8	6.4
1.0	6.68	0.544	16.0	16.3
2.0	3.34	0.588	1.9	2.4
2.0	5.01	0.561	4.1	4.5
2.0	5.01	0.561	3.3	4.3
2.0	6.68	0.544	8.4	8.9
2.0	6.68	0.544	6.6	7.0
3.0	8.35	0.536	11.5	10.8
4.0	6.68	0.544	1.3	1.5
4.0	8.35	0.536	2.8	3.1
4.0	10.02	0.538	3.3	3.0
5.0	6.68	0.544	1.0	0.83
8.0	10.02	0.538	0.6	0.47
10.2			0.0	0.0

equation (80), with $\mathcal{P}_{xy}(l, t)$ and $\mathcal{P}_z(l, t)$ given by equations (71) and (79), respectively, the velocities $v_{0\text{max}}$, v_{0m} , v_{lc} , and v_{0zm} being expressed, in order, by equations (60), (156), (70), and (78). In our equations, there are three unknown parameters, namely ρ , $\zeta = n_{ei}n_{ie}$, and \mathcal{T} , which are important microscopic quantities at the extreme temperatures and conditions of the electrical discharges, at present not obtainable by any other method. Actually, ρ , appearing in equation (12), gives the contribution to the number f of ionized electrons per atoms due to the current I ; $\zeta = n_{ei}n_{ie}$, appearing in equation (80), is the product of n_{ei} (number of ions extracted by one electron) and n_{ie} (number of electrons extracted by one ion); \mathcal{T} , appearing in equation (164), expresses the relaxation time at which the small range of speeds just before v_{0m} is practically reconstructed. Now a ρ value is necessary to calculate the time t^* [appearing in Eq. (90)] at which the process of the run-aways starts. We have therefore adopted an iterative procedure putting, at zero order, $\rho = 0$ in Section 3.1, thus obtaining equation (47). It is with the t^* given by equation (47), and used in equation (90), that we have made a data fitting with the experimental data of Graneau et al. [1]. We find the correct dependence of h on the value l_1 of the smaller gap, and a good numerical equality to the experimental data provided the three sought parameters take the following first order values

$$\rho_1 = 1.46 \times 10^{-6} \text{ A}^{-1}; \quad \zeta_1 = 0.21; \quad \mathcal{T}_1 = 88 \mu\text{s}. \quad (93)$$

With this ρ_1 value in equation (12), and the same procedure of Section 3.1, we find the new t_2^* values that can be expressed by

$$t_2^*(C) \simeq 0.672 - 0.206(C/6.68) + 0.078(C/6.68)^2, \quad (94)$$

where C is measured in μF and t_2^* in μs .

We see that the t_2^* values given by equation (94) differ of only some percents from those given by equation (47). With the new t_2^* , the data fitting with the experimental data is shown in Table 2, and the second order values of

the three important microscopic parameters are

$$\rho_2 = 1.41 \times 10^{-6} \text{ A}^{-1}; \quad \zeta_2 = 0.22; \quad \mathcal{T}_2 = 86 \mu\text{s}. \quad (95)$$

We see that these values little differ from those of equation (93), showing that our iterative procedure converges very rapidly.

The found \mathcal{T} value deserves a comment. The usual relaxation time in the case of binary collisions between electrons and atoms (either neutral or ionized) is of the order $t_{\text{relax}} = \nu^{-1}(v_m)M/(2m)$, where $\nu^{-1}(v_m)$ has to be taken in correspondence of roughly twice the minimum value v_{rm} to have run-aways and given by equation (159) of Appendix B.2. With the value $v_{rm} = 3.02$ derived four lines after equation (162), and the use of equation (104) of Appendix A with $v_r = 2v_{rm}$, we derive

$$\nu^{-1}(2v_{rm}) \simeq 10^{-11} \text{ s}. \quad (96)$$

Consequently, with $M/2m \simeq 1836 \times 7 \simeq 10^4$ we obtain

$$t_{\text{relax binary}} \simeq 10^{-7} \text{ s}. \quad (97)$$

To have found the value given by equation (95) means that triple collisions are necessary to reconstruct the high velocity tail of the electron distribution function. Obviously, binary collisions are widely dominant for lower v values, i.e., for $0 \leq v \leq 1.8\langle v^2 \rangle^{1/2}$. Actually, as calculated in Appendix B, the minimum value to have run-away electrons, is $v_{0m} = 2.45 \times 10^6$ m/s, while, at the discharge temperature $\simeq 4 \times 10^4$ K, it is $\langle v^2 \rangle^{1/2} = (3kT/m)^{1/2} = 1.35 \times 10^6$ m/s, so that $v_{0m}/\langle v^2 \rangle^{1/2} \simeq 1.8$.

6 Conclusions

It would have been practically impossible to conceive an experiment as the one performed by Graneau et al. [1] in order to derive the three microscopic parameters ρ , $\zeta = n_{ei}n_{ie}$, and \mathcal{T} . It is a case of ‘‘heterogenesis of aims’’. Actually, Graneau et al. [1] devised their own experiment to validate Ampère’s expression, but the correct, although rough, interpretation [2] of their effect, has on the contrary validated the standard formula of Grassmann. The point is that the much deeper (with respect to Ref. [2]) interpretation given in this paper includes the above three parameters that has been determined by data fitting. Notice that the experimental points are 15, so that the agreement with the two main dependences, namely on the smaller gap length l_1 , and on the maximum amplitude I_0 of the current (related to the value of the capacitance C), are a proof of the correctness of our interpretation. Let us clarify this point. The dependence of the maximum upward displacement h of the mobile armature on I_0 (or on C) is determined by the expression of the number f of extracted electron per atom. The general expression is rather easy to be devised because it must reduce to the thermal expression f_T for $I_0 \rightarrow 0$, and must be limited to 7 (number of electron of one atom of nitrogen) for $I \rightarrow \infty$. The wanted expression is equation (12) where an unknown parameter

ρ appears. It is very difficult to find ρ theoretically so that we have left it as one of the three unknown parameters. The data fitting has given $\rho = 1.41 \times 10^{-6} \text{ A}^{-1}$ (since ρI must give a number, and I is measured in A, then the dimension of ρ is in A^{-1}).

The dependence of h on l_1 is correctly given by our theory based on the run-away electrons and ions. An unknown parameter contained in it is $\zeta = n_{ei}n_{ie}$ where n_{ei} (or n_{ie}) is the number of ions (or electrons) extracted from an electrode by one electron (or ion). In the extreme conditions of the electrical discharge there have been so far neither theory nor experiment able to determine it. Our data fitting has produced $\zeta = n_{ei}n_{ie} = 0.22$. In Section 4 we have also suggested a modified version of the Graneau et al. [1] experiment by which it would be possible to separately derive n_{ei} and n_{ie} .

The third parameter we have obtained is the average time \mathcal{T} of relaxation to reconstruct the high energy tail of the electron distribution function. We have found a single paper [4] that gives information in the case of cross-sections $\propto v^{-1}$ (hence constant collision frequency ν), and $\propto v^{-3}$ (hence $\nu \propto v^{-2}$), which are never found in any material in all the v range. Our data fitting have given $\mathcal{T} \simeq 8.6 \times 10^{-5} \text{ s}$ [as given by Eq. (95)], i.e., a rather long time compared to the relaxation time for binary collisions which, in discharge conditions, is of the order 10^{-7} s , as given by equation (97). This is a sign that at least triple collisions are required to produce the high velocities in the distribution function. Actually, with binary collisions between particles having the same mass, we have at maximum (for head-on collisions) an exchange of their speeds. To gain speed, an electron has to collide against two other electrons having roughly the same velocities. Our result is therefore sensible. We stress that no other method or theory is at present able to give the order of magnitude of \mathcal{T} , not even in principle. At first sight one could think that modern experiments that study discharges, especially those based on laser and imaging techniques, could produce good values for the three parameters we have obtained. Actually, the laser experiments are far superior than any electro-mechanical experiment, primarily because of timing and spatial resolutions. But they are “blind” with respect to run-away electrons, while Graneau et al. experiment detects them (practically, it “sees” only run-away electrons). Perhaps, in some indirect way the laser experiments could give some values regarding the first two parameters, ρ (regarding the additional ionization due to the electric current), and ζ [number of ions (electrons) extracted by one electron (ion)]. But it seems that they are unable in principle to produce any \mathcal{T} value. The latter is also the most important, because it is required in the theory, we have just developed [3], that explains for the first time the long standing problem of the practically infinite memory of a fluctuation in the conduction current. The correlation function decays as $t^{-0.005}$ leading to a power spectral density of the fluctuating conductance G given by

$$S_G(\omega) = \frac{G^2 \alpha_\varepsilon}{2\pi \mathcal{N} \omega^{-0.995}}, \quad (98)$$

where \mathcal{N} is the number of electrons between the sample electrodes, ω the angular frequency, and α_ε a coefficient that, differently from Hooge’s empirical formula, depends on the electron concentration N . It is this dependence, together with the \mathcal{T} value given in this paper, that leads to a close fitting with the experimental data.

We again encourage Graneau and collaborators to improve and modify their experiment whose correct interpretation can open a new stream of research.

Appendix A: Plasma conductivity σ and attenuation distance δ of e.m. waves during the discharge

In order to calculate the coefficient A appearing in equation (19) we must evaluate the attenuation length δ in the ionized air during a discharge.

The attenuation of a plane wave may be expressed in terms of the real and imaginary parts of the wave number k , by equation (7.53) of reference [10]

$$k = \beta + i\alpha/2 \quad (99)$$

where the parameter α is known as the attenuation constant or absorption coefficient. The intensity of the wave falls off as $\exp(-\alpha x)$.

If the fields associated with the radiation vary in space and time as $\exp[i(\mathbf{k} \cdot \mathbf{x} - \omega t)]$, the wave number k is given by the complex expression (7.68) of reference [10] (here translated into the International System)

$$k = \sqrt{\mu\varepsilon} \frac{\omega l}{c} \left(1 + i \frac{\sigma}{\omega l \varepsilon} \right)^{1/2}, \quad (100)$$

ε being the dielectric constant, μ the permeability, and σ the conductivity. Comparing equation (99) with equation (100), and translating equation (7.69) of reference [10] into the International System [11], it follows that

$$\alpha = \frac{\omega l}{c} \sqrt{2\varepsilon_r \mu_r} \left[\sqrt{1 + \left(\frac{\sigma}{\omega l \varepsilon_0 \varepsilon_r} \right)^2} - 1 \right]^{1/2}, \quad (101)$$

where ε_0 is the vacuum permittivity and, for a plasma, $\varepsilon_r \simeq \mu_r \simeq 1$. The conductivity can be related to the drift velocity \mathbf{w} for electrons via [12]

$$\mathbf{j} = \sigma \mathbf{E} = Ne\mathbf{w} = Ne \frac{e\mathbf{E}}{m} \left\langle \frac{1}{\nu} - \frac{v}{3\nu^2} \frac{d\nu}{dv} \right\rangle, \quad (102)$$

where N is the concentration, ν the collision frequency for momentum transfer, and the sign of average means that the enclosed expression has to be averaged over the normalized distribution function of the thermal speed v of electrons. The total collision frequency ν for momentum transfer appearing in equation (102) is the sum of three contributions, namely, the electron-ion contribution ν_i , the electron-atom contribution ν_a , and the photon-scattering contribution ν_p

$$\nu = \nu_i + \nu_a + \nu_p. \quad (103)$$

The ν_i for electrons in ions is given by the Brooks-Herring expression and we refer to Appendix A.3 of reference [8] for recent calculations. The final expression, taken from equation (A.19) of reference [8] is

$$\nu_i = \frac{Ne^4}{8\pi\epsilon_0^2 m^2 v_r^3} \left(\frac{m}{2kT}\right)^{3/2} \left[\ln(1+b) - \frac{b}{b+1} \right], \quad (104)$$

where v_r is the reduced speed

$$v_r = v (m/2kT)^{1/2}, \quad (105)$$

and b is given by equation (A.16) of reference [8]

$$b = \frac{4\epsilon_0 kT m^2 v^2}{\hbar^2 e^2 N} = \frac{8\epsilon_0 m}{\hbar^2 e^2 N} (kT)^2 v_r^2. \quad (106)$$

The collision frequency for momentum transfer given by equation (104) is not valid for $b < 10$ and implies a non-physical divergence for $v_r \rightarrow 0$. We should limit it to $b \geq 10$ and then use the convenient extrapolation given by equation (A.20) of reference [8]. However, since we are interested in the $\langle 1/\nu_i(v) \rangle$ appearing in equation (102) and in the drift velocity, given by equation (5), we can use equation (104) since the tail for $v_r \rightarrow 0$ (which implies the divergence of ν_i) gives an almost negligible difference to the average with respect to the result derivable from equation (A.20) of reference [8].

As shown in Appendix B, practically each atom is singly ionized so that we have put $Z = 1$ in equation (A.19) of reference [8]. The effective mass m^* in solids is here the electron mass m . At the beginning of the discharge, before the air in the gaps expands, the molecule concentration is twice the atmospheric one since all the diatomic air molecules are immediately dissociated in two monoatomic molecules

$$N_0 = 2N_a = 5.4 \times 10^{25} \text{ m}^{-3}, \quad (107)$$

so that equation (106) becomes, with the ‘‘a posteriori’’ estimated value for the average discharge temperature $T \simeq 4.2 \times 10^4$ K [as given by Eq. (26)]

$$b = 1.42 \times 10^3 v_r^2. \quad (108)$$

For simplicity, we take a Maxwellian distribution at the temperature calculated in Section 3 (the Chapman-Cowling-Davidov distribution does not take into account the losses due to radiation)

$$\begin{aligned} f_0(v) &= \left(\frac{m}{2\pi kT}\right)^{3/2} \exp\left(-\frac{mv^2}{2kT}\right) \\ &= \left(\frac{m}{2\pi kT}\right)^{3/2} \exp(-v_r^2). \end{aligned} \quad (109)$$

We obtain therefore

$$\begin{aligned} \left\langle \frac{1}{\nu_i} \right\rangle &= \int_0^\infty dv 4\pi v^2 f_0(v) \nu_i^{-1} = 64\epsilon_0^2 (2\pi m)^{1/2} \frac{(kT)^{3/2}}{N_0 e^4} \\ &\times \int_0^\infty dv_r v_r^5 \exp(-v_r^2) \left[\ln(1+b) - \frac{b}{b+1} \right]^{-1}. \end{aligned} \quad (110)$$

Numerical integration of equation (110) with the use of equation (109) leads to

$$\left\langle \frac{1}{\nu_i} \right\rangle = 8.94\epsilon_0^2 (2\pi m)^{1/2} \frac{(kT)^{3/2}}{N_0 e^4} \simeq 2.09 \times 10^{-14} \text{ s}. \quad (111)$$

The average collision frequency $\langle \nu_i^{-1} \rangle^{-1} \simeq 4.8 \times 10^{13} \text{ s}^{-1}$. Up to a temperature $T < 1000$ K, the average collision frequency ν_a with atoms considered as neutral is

$$\langle \nu_a \rangle = \langle N\pi r_{at}^2 v \rangle \simeq 7 \times 10^{12} \text{ s}^{-1}, \quad (112)$$

which is smaller than the ion-electron collision frequency ν_i even at small temperatures. For $T > 1000$ K the neutral atom-electron collision frequency decreases until it becomes negligible at the ionization temperature.

To calculate ν_p with photons we must calculate the average amplitude E of the electric field of the radiating light. At the discharge temperature $\simeq 4.2 \times 10^4$ K, the energy density U of the e.m. radiation field can be derived from the Stefan-Boltzmann law $p_{\text{rad}} = \sigma T^4$ and the relationship $p_{\text{rad}}/c = U$, i.e.

$$U = \epsilon_0 E^2 = \sigma T^4 / c \simeq 588 \text{ Jm}^{-3}, \quad (113)$$

whence

$$E = \left(\frac{588}{8.85 \times 10^{-12}} \right)^{1/2} = 8.2 \times 10^6 \text{ Vm}^{-1}. \quad (114)$$

The variation of velocity in half a period π/ω_l , where ω_l is the angular frequency of the radiating light we take in correspondence of the maximum of the Planck curve, i.e., $\omega_l \simeq 10^{16} \text{ s}^{-1}$, is

$$\Delta v \simeq \frac{eE}{m} \frac{\pi}{\omega_l} \simeq 450 \text{ ms}^{-1}, \quad (115)$$

which is therefore much smaller than the average thermal speed of an electron at the discharge temperature, that is $\langle v^2 \rangle^{1/2} \simeq 1.4 \times 10^6 \text{ m/s}$. It follows that the collision frequency ν_p is negligible compared to the collision frequency with ions, which is practically the only one effective at high temperature. We therefore take equation (104) as the total collision frequency. It is therefore $\nu \propto v^{-3}$ and, substituting equations (104), (107), and (111) into equation (102), we obtain

$$\sigma \simeq 2N_0 \frac{e^2}{m} \left\langle \frac{1}{\nu_i} \right\rangle = 6.35 \times 10^4 \text{ m}^{-1} \Omega^{-1}. \quad (116)$$

The term inside the square root of equation (101) takes therefore the value, for blue light for which $\lambda \simeq 0.5 \mu\text{m}$, whence $\omega_l = 2\pi c/\lambda \simeq 3.8 \times 10^{15} \text{ s}^{-1}$,

$$\frac{\sigma}{\omega_l \epsilon_0} \simeq 1.9. \quad (117)$$

Substituting equation (117) into equation (101) we obtain the attenuation distance

$$\delta = \alpha^{-1} = 5.24 \times 10^{-8} \text{ m}. \quad (118)$$

We have this small value at the beginning of the discharge. Even when, because of the expansion, $N = N_0/86$, we have

$$\delta \simeq 3.6 \times 10^{-6} \text{ m} \ll r_g. \quad (119)$$

The plasma remains always opaque and the radiation comes practically from the external surface of the discharge column, as expressed in equation (19). The coefficient A appearing in equation (19) is practically constant and, for air, it is $A \simeq 0.4$ (roughly 0.4 of the value for a black body).

Appendix B: Number of electrons and ions in run-away that impinge on the face of the mobile section

We begin to calculate the ratio N_i/N_e , where N_i and N_e are the concentrations of the ions and free electrons, respectively. As soon as the discharge starts, the air molecules are split into atoms which are partially ionized. If the atoms were singly ionized it would be $N_e = N_i$. If twice ionized $N_e = 2N_i$. The fraction f_T of ionized atoms is given by equation (10). The first ionization energies for oxygen (O) and nitrogen (N) are $\varepsilon_{iO1} = 13.62 \text{ eV} = 2.18 \times 10^{-18} \text{ J}$ and $\varepsilon_{iN1} = 14.53 \text{ eV} = 2.33 \times 10^{-18} \text{ J}$, respectively [13]. (It is $1 \text{ eV} = 1.60219 \times 10^{-19} \text{ J}$, equivalent to a temperature $T_{\text{eq}} = 1.1605 \times 10^4 \text{ K}$.) For the minimum ($C = 3.34 \mu\text{F}$) and maximum ($C = 10.02 \mu\text{F}$) values of capacitance, the peak temperatures range from $4.34 \times 10^4 \text{ K}$ to $4.37 \times 10^4 \text{ K}$. Then equation (10) leads to the following ranges for f_{Ts} relevant to O and N, respectively. For $s = 1$ (first ionization) we obtain

$$\begin{aligned} 0.026 &\leq f_{TO1} \leq 0.027; \\ 0.020 &\leq f_{TN1} \leq 0.021. \end{aligned} \quad (120)$$

The energies of second ionization are $\varepsilon_{iO2} = 35.12 \text{ eV} = 5.62 \times 10^{-18} \text{ J}$ and $\varepsilon_{iN2} = 29.59 \text{ eV} = 4.74 \times 10^{-18} \text{ J}$, respectively. The corresponding ranges for f are

$$\begin{aligned} 8.4 \times 10^{-5} &\leq f_{TO2} \leq 8.9 \times 10^{-5}; \\ 3.6 \times 10^{-4} &\leq f_{TN2} \leq 3.9 \times 10^{-4}, \end{aligned} \quad (121)$$

respectively. Comparing equation (120) with equation (121) we obtain

$$\begin{aligned} 3.2 \times 10^{-3} &\leq f_{TO2}/f_{TO1} \leq 3.3 \times 10^{-3}; \\ 1.8 \times 10^{-2} &\leq f_{TN2}/f_{TN1} \leq 1.9 \times 10^{-2}. \end{aligned} \quad (122)$$

Since the above ratios are less than two percents, we can take $N_i \simeq N_e$.

For simplicity, in the main text we have taken a single, effective value for the ionization energy of an ‘‘air’’ atom, so as to obtain the same value of the total ionization for oxygen and nitrogen taking into account their first and second ionization energies and their ratio in air. The effective value is $\varepsilon_i = 14.06 \text{ eV} = 2.25 \times 10^{-18} \text{ J}$.

To calculate the electron and ions in run-away we need the values of their mean free paths, related to the collision

frequency ν_c . Notice that the collision frequency of interest in this case is not the ν_i given by equation (104), which is the one relevant to the momentum transfer and has been integrated over the cosine μ_{sc} of the scattering angle θ_{sc} . We are here interested in the collision frequency given by equation (22) of reference [8] we report here

$$\nu_c = \frac{Ne^4}{16\pi^2\varepsilon_0^2g^3m_r^2} \left(1 - \mu_{sc} + \frac{\hbar^2\beta_s^2}{2g^2m_r^2}\right)^{-2}, \quad (123)$$

where N is the concentration for either ions or electrons, e the electron charge, ε_0 the vacuum permittivity, g the absolute value of relative velocity, m_r the reduced mass, $\mu_{sc} = \cos\theta_{sc}$ the cosine of the scattering angle, \hbar the reduced Planck constant, and

$$\beta_s^2 = \frac{Ne^2}{\varepsilon_0kT} \frac{F_{-1/2}}{F_{+1/2}}, \quad (124)$$

$F_{-1/2}$ and $F_{+1/2}$ being the Fermi-Dirac integrals. The collision frequency ν_c is very high at small θ_{sc} corresponding to $\mu_{sc} \simeq 1$. However, small deviation are ineffective for our purposes of calculating the deviations of trajectories, so that we eliminate the scattering angles between 0 and $\sim 30^\circ$. The average ν_c value in the remaining θ_{sc} interval corresponds to $\theta_{sc} \simeq \pi/2$, i.e., to $\mu_{sc} = 0$. For simplicity we take this value which is just what assumed in the simplified distribution $g_2(v_0)$ given by equation (65). Consequently, we take as effective mean free path

$$\lambda = \frac{g}{\nu_c} \simeq \frac{16\pi^2\varepsilon_0^2g^4m_r^2}{Ne^4}, \quad (125)$$

having neglected the third term inside the round bracket of equation (123) since it is $\ll 1$. Taking into account that, because of axial symmetry, there is the weight $\sin\theta_{sc}$ which is maximum for $\theta_{sc} = \pi/2$ corresponding to $\mu_{sc} = 0$, we can take the expression given by equation (125) for any θ_{sc} value. In the case of electron-ion scattering, the relative speed g is practically equal to the electron speed v , and the reduced mass m_r is quite close to the electron mass m . Consequently, equation (125) becomes

$$\lambda_{e\text{-ion}} \simeq \frac{16(\pi\varepsilon_0m)^2}{Ne^4}v^4. \quad (126)$$

For electron-electron scattering, $m_r = m/2$ and considering equal velocities v for the two colliding electrons,

$$\langle g^4 \rangle_{\theta_{sc}} = \int_0^\pi d\theta_{sc} \frac{1}{2} \sin\theta_{sc} (v^2 + v^2 - 2v^2\cos\theta_{sc})^2 = \frac{16}{3}v^4, \quad (127)$$

so that equation (125) becomes, with the use of equation (127),

$$\lambda_{e\text{-e}} \simeq \frac{32(\pi\varepsilon_0m)^2}{Ne^4}v^4. \quad (128)$$

The collision frequencies due to both e-e and e-ion scatterings add each other so that the resulting free path, being the concentration N of electrons equal to that of the ions, is given, with the use of equations (126) and (128), by

$$\lambda_e = \frac{\lambda_{e\text{-ion}}\lambda_{e\text{-e}}}{\lambda_{e\text{-ion}} + \lambda_{e\text{-e}}} \simeq \frac{32(\pi\varepsilon_0m)^2}{5Ne^4}v^4. \quad (129)$$

When an ion interacts with an electron it does not practically deviate. What is effective is the ion-ion scattering whose mean free path $\lambda_{\text{ion-ion}}$ turns out to be equal to λ_{e-e} given by equation (128) (now with the ion mass M and velocity u for m and v).

We can now calculate what is the minimum value of the initial velocities so that the mean free paths overcome the lengths of the gaps. At first sight it would seem that this condition is very different for the smaller gap (measurements performed by Graneau et al. [1] down to $l_1 = 1$ mm) than for the larger gap (up to $\simeq 20$ mm). The point is that the electric field in the gaps is very high. The value of the electric field E can be derived from equation (2) and is

$$E = \frac{RI}{l} = \frac{R}{l} \left(\frac{\langle P \rangle}{R} \right)^{1/2} = \frac{R}{l} \varphi_0 \sqrt{\frac{C}{2L}} \exp\left(-\frac{t}{\tau}\right), \quad (130)$$

where $l = 2.05 \times 10^{-2}$ m. For $C = 6.68 \mu\text{F}$ and $t = t_g$ given by equation (43) we obtain $E(t_g) \simeq 1.4 \times 10^5$ V/m. With this high E values, as soon as an electron (or an ion) mean free path λ_e overcomes 0.2 mm in the field direction, its acquired energy is $\simeq 26$ eV, roughly five times the average energy at the beginning of the discharge ($\simeq 4.6$ eV). Since $\lambda_e \propto v_r^4$ [as given by equation (129)] and $v_r^2 \propto E$, its λ_e becomes 100 times the initial value 0.2 mm, that is 20 mm, the length of the larger gap. Actually, after $\lambda_e > 2$ mm the energy that it could acquire with the same conditions would be 100 times the initial energy, and λ_e would become $10^4 \times 0.2$ mm = 2 m. In other terms, the electron becomes collisionless and acquire more and more energy from E . This condition is called “run-away”. Consequently, as soon as an electron becomes run-away, its mean free path increases indefinitely. Let us evaluate the fraction, or probability p_r , of the run-away electrons.

To obtain the minimum initial speeds that lead to run-aways we proceed as follows, distinguishing different cases.

B.1 Minimum initial speed v_{0m} to have run-aways for electron extracted parallel to the bases of the gaps

Having assumed the simplified distribution $g_2(v_0)$ given by equation (65) of the initial velocities v_0 with $\mathbf{v}_0 \cdot \mathbf{a} = 0$ (transversal velocities with respect to the acceleration \mathbf{a}), the velocity acquired by an electron after time t is

$$v^2 = v_0^2 + a^2 t^2. \quad (131)$$

The minimum initial speed v_{0m} is obtained imposing that the acquired speed v in a mean free time $\langle t \rangle(v_{0m})$ be such that the corresponding λ_e is equal to the total length l of the gaps, i.e.,

$$\bar{v}^2 = v_{0m}^2 + a^2 \langle t(v_{0m}) \rangle^2, \quad (132)$$

where \bar{v} can be derived from equation (129) where we set $\lambda_e = l$,

$$\bar{v} = \left[\frac{5Ne^4 l}{32(\pi\epsilon_0 m)^2} \right]^{1/4}. \quad (133)$$

The mean free time $\langle t \rangle$ corresponding to v_{0m} is obtained from

$$\lambda_m = \int_0^{\langle t \rangle} dt (v_{0m}^2 + a^2 t^2)^{1/2} = \frac{\langle t \rangle}{2} \sqrt{v_{0m}^2 + a^2 \langle t \rangle^2} + \frac{v_{0m}^2}{2a} \sinh^{-1} \left(\frac{a \langle t \rangle}{v_{0m}} \right). \quad (134)$$

In all our cases we find $v_{0m} < \bar{v}/2.5$ so that the second term of the last side of equation (134) is less than 0.3 times the first term. Neglecting it for simplicity, we obtain

$$\langle t \rangle = 2\lambda_m/\bar{v}. \quad (135)$$

We can assimilate the mean free path λ_m to the λ_e given by equation (129), corresponding to $v = \text{constant} = v_{0m}$. Substituting equations (129) and (135) into equation (132) we obtain

$$v_{0m}^8 + v_{0m}^2 q - \bar{v}^2 q = 0, \quad (136)$$

where

$$q = \frac{\bar{v}^2}{4a^2} \left[\frac{5Ne^4}{32(\pi\epsilon_0 m)^2} \right]^2. \quad (137)$$

Setting $v_{0m}^2 = x$ we obtain an equation of fourth degree in canonical form

$$x^4 + px^2 + qx + r = 0 \quad (138)$$

where

$$p = 0, \quad q \text{ as given by equation (137), } r = -q\bar{v}^2. \quad (139)$$

The connected equation of third degree (Euler's resolvent) is in our case

$$z^3 + \frac{q}{4}\bar{v}^2 z - \frac{q^2}{64} = 0, \quad (140)$$

whose solutions are

$$z_1 = Y - \frac{q\bar{v}^2}{12Y}, \quad (141)$$

$$z_2 = Y \exp\left(i\frac{2\pi}{3}\right) - \frac{q\bar{v}^2}{12Y} \exp\left(-i\frac{2\pi}{3}\right) = \eta \exp(i \arctan Z) \quad (142)$$

$$z_3 = Y \exp\left(-i\frac{2\pi}{3}\right) - \frac{q\bar{v}^2}{12Y} \exp\left(i\frac{2\pi}{3}\right) = \eta \exp(-i \arctan Z) \quad (143)$$

where

$$Y = \left\{ \frac{q^2}{128} + \left[\left(\frac{q^2}{128} \right)^2 + \frac{1}{27} \left(\frac{q}{4}\bar{v}^2 \right)^3 \right]^{1/2} \right\}^{1/3}, \quad (144)$$

$$\eta = \left[Y^2 \left(\frac{q\bar{v}^2}{12Y} \right)^2 + \frac{q\bar{v}^2}{12} \right]^{1/2}, \quad (145)$$

$$Z = -\frac{1.732}{z_1} \left(Y + \frac{q\bar{v}^2}{12Y} \right) \quad (146)$$

The solution of equation (138) is then

$$x = \sqrt{z_1} + \sqrt{z_2} + \sqrt{z_3}, \quad (147)$$

with the signs of the radicals determined by the condition

$$\sqrt{z_1}\sqrt{z_2}\sqrt{z_3} = -\frac{q}{8}. \quad (148)$$

Precisely, being z_2 and z_3 complex numbers, we denote

$$y_1(k=0) = z_1^{1/2} \exp\left(i\frac{2k\pi}{2}\right) = \left(Y - \frac{q\bar{v}^2}{12Y}\right)^{1/2}, \quad (149)$$

$$y_1(k=1) = -z_1^{1/2} \exp(ik\pi) = -\left(Y - \frac{q\bar{v}^2}{12Y}\right)^{1/2}, \quad (150)$$

$$y_2(k=0) = \eta^{1/2} \exp\left(\frac{i}{2} \arctan Z\right), \quad (151)$$

$$y_2(k=1) = \eta^{1/2} \exp\left[i\left(\pi + \frac{1}{2} \arctan Z\right)\right], \quad (152)$$

$$y_3(k=0) = \eta^{1/2} \exp\left(-\frac{i}{2} \arctan Z\right), \quad (153)$$

$$y_3(k=1) = \eta^{1/2} \exp\left[i\left(\pi - \frac{1}{2} \arctan Z\right)\right]. \quad (154)$$

Since $x = \bar{v}_{0m}^2 > 0$, there is only one positive real solution given by

$$x = v_{0m}^2 = y_1(k=1) + y_2(k=0) + y_3(k=0). \quad (155)$$

Finally, with the use of equations (150), (151), and (153) we obtain

$$v_{0m} = \sqrt{x} = \left[-z_1^{1/2} + 2\eta \cos\left(\frac{1}{2} \arctan Z\right)\right]^{1/2}, \quad (156)$$

where z_1 is given by equation (141), η by equation (145), and Z by equation (146).

Reading from Table 1, for $C = 6.68 \mu\text{F}$, we have $N(r=0, t=t^*) = 6.25 \times 10^{23} \text{ m}^{-3}$, and, with the E value just after equation (130), $a(t_0) = eE/m = 2.5 \times 10^{16} \text{ ms}^{-2}$ so that, with $l = 20.2 \times 10^{-3} \text{ m}$, we derive $\bar{v} = 6.7 \times 10^6 \text{ ms}^{-1}$ from equation (133), $q = 1.78 \times 10^{28} \text{ m}^6\text{s}^{-6}$ from equation (136), $Y = 2.59 \times 10^{25} \text{ m}^4\text{s}^{-4}$ from equation (144), $z_1 = 1.91 \times 10^{23} \text{ m}^4\text{s}^{-4}$ from equation (141), $\eta = 2.58 \times 10^{25} \text{ m}^4\text{s}^{-4}$ from equation (145), $Z = -468$ from equation (146). By these values we obtain from equation (156) $v_{0m} = \sqrt{x} = 2.45 \times 10^6 \text{ ms}^{-1}$. We have taken, in the above example, $N = N(r=0, t^*) = 6.25 \times 10^{23} \text{ m}^{-3}$. If we take $N' = 1.2N(r=0, t_g) = 7.5 \times 10^{23} \text{ m}^{-3}$ we obtain $v'_{0m} = 5.13 \times 10^6 \text{ ms}^{-1} > v_{\text{max}lc}$. If we take $N'' = 1.1N(r=0, t_g) = 6.87 \times 10^{23} \text{ m}^{-3}$ we obtain $v''_{0m} = 3.38 \times 10^6 \text{ ms}^{-1}$ which gives a small value for $\mathcal{P}_{e,xy}$ and \mathcal{P}_z expressed by equations (71) and (79), respectively.

Consequently, since $N(r)$ given by equation (57) rapidly tends to $N(r=0, t_g)$ for small $r - r_g$ values, we take that the source of run-away is uniform from $r=0$ to r_{max} at which $N = 1.1N(r=0, t_g)$, and then 0, i.e., the distribution $q(r)$ appearing in equation (71) is given by

$$q(r) = \frac{2}{r_{\text{max}}^2} \Theta(r_{\text{max}} - r). \quad (157)$$

B.2 Numerical run-away current

We first evaluate the fraction, or probability p_r , of the run-away electrons. Let us denote by t the flight time and by θ the angle between the initial velocity \mathbf{v}_0 of an electron just after a scattering and its acceleration $\mathbf{a} = e\mathbf{E}/m$. The velocity v acquired after t by an electron in uniformly accelerated motion is

$$v^2 = v_0^2 + a^2 t^2 + 2av_0 t \cos \theta. \quad (158)$$

For $\theta > \pi/2$ the velocity v decreases (with respect to v_0), λ_e becomes shorter and a collision interrupts a possible run-away. For $0 \leq \theta \leq \pi/2$ it is $v(t) > v_0$ and if the electron succeeds to become a run-away for $\theta = \pi/2$, to a greater extent it succeeds if $\theta < \pi/2$. We take as the minimum value to have run-aways the v_{0m} expressed by equation (156). Here it is convenient to use its relative value as given by equation (105), i.e.,

$$v_{rm} = v_{0m} [m/2kT(t \geq t_0)]^{1/2}. \quad (159)$$

Consequently, we calculate the probability p_r to have run-aways as half the number of electrons with initial reduced velocities [defined by equation (105)] larger than the minimum value v_{rm} to have run-aways. It is, taking a Maxwellian distribution of velocities

$$\begin{aligned} p_r &= \frac{2}{\sqrt{\pi}} \int_{v_{rm}}^{\infty} dv_r v_r^2 \exp(-v_r^2) \\ &= \frac{1}{\sqrt{\pi}} v_{rm} \exp(-v_{rm}^2) + \frac{1}{2} \text{erfc}(v_{rm}), \end{aligned} \quad (160)$$

where the normalization is assured by

$$1 = \frac{4}{\sqrt{\pi}} \int_0^{\infty} dx x^2 \exp(-x^2). \quad (161)$$

The factor 2 in the intermediate step of equation (160), instead of the 4 of the second step of equation (161), is due to having taken half of the electrons. Indeed, since the electrons velocities are practically isotropically distributed, to have assumed as effective the \mathbf{v}_0 forming with \mathbf{a} an angle $0 \leq \theta \leq \pi/2$ means to take, as effective, half the number of electrons.

The number of run-aways in the two gaps is therefore

$$\mathcal{N} = 2p_r f N_{\text{out}} r_g^2 (l_1 + l_2), \quad (162)$$

where the factor 2 implies the sum of electrons and ions and f the number of free electrons due to ionization and given by equation (12).

For $C = 6.68 \mu\text{F}$ it is $N_{\text{out}} = 3.55 \times 10^{25} \text{ m}^{-3}$, $T(t^*) = 4.08 \times 10^4 \text{ K}$, so that we derive $v_{rm} = 3.06$ from equation (159), $p_r \simeq 0.127$ from equation (160), and $\mathcal{N} \simeq 5.16 \times 10^{16}$ from equation (162).

The point is: in how much time do the electrons and ions reconstruct the high energy tail of the distribution function for $v \geq v_{0m}$? Actually the \mathcal{N} electrons and ions that becomes run-away are rapidly swept away by the

electric field E . What is important is therefore the relaxation time \mathcal{T} at which the small range of relative speeds $(1 - \delta)v_{0m} \leq v \leq v_{0m}$ is practically reconstructed. Then the run-away current is

$$I_{\text{run}} = \frac{d\mathcal{N}}{dt} \simeq \frac{\mathcal{N}}{\mathcal{T}}. \quad (163)$$

To find \mathcal{T} theoretically is extremely difficult and the error can be very large. We therefore leave \mathcal{T} as the third unknown parameter to be determined by data fitting. With the use of equations (162) and (163), the run-away current is therefore expressed by

$$I_{\text{run}} = \frac{2}{\mathcal{T}} p_r f N_{\text{out}} r_g (l_1 + l_2), \quad (164)$$

where p_r is given by equation (160), f by equation (12), and N_{out} by equation (51).

References

1. N. Graneau, T. Phipps, D. Roscoe, Eur. Phys. J. D **15**, 87 (2001)
2. G. Cavalleri, E. Cesaroni, E. Tonni, G. Spavieri, Eur. Phys. J. D **26**, 221 (2003); see also: G. Cavalleri, G. Bettoni, E. Tonni, G. Spavieri, Phys. Rev. E **58**, 2505 (1998); G. Cavalleri, E. Tonni, Phys. Rev. E **62**, 7545 (2000); G. Cavalleri, E. Tonni, G. Spavieri, Phys. Rev. E **63**, 058602 (2001)
3. G. Cavalleri, L. Bosi, Phys. Stat. Sol. (c) **4**, 1230 (2007)
4. M. Krook, T. Tsun Wu, Phys. Rev. Lett. **36**, 1107 (1976)
5. At the ignition of the discharge the volume of the air inside the discharge remains practically constant (thus keeping its initial volume). The specific heat per unit mass at constant volume of non dissociated air is $c_{m \text{ non}} = 714 \text{ J (kg K)}^{-1}$. For dissociated air c_m , being proportional to the degrees of freedom that reduce from 6 to 3, is reduced with a factor 2.
6. <http://www.webelements.com/webelements/elements/text/N/radii.html>
7. H. Brooks, Phys. Rev. **83**, 879 (1951); *Advances in Electronics and Electron Physics*, edited by L. Marton (Academic Press, New York, 1955), Vol. 7, p. 85; C. Herring, E. Vogt, Phys. Rev. **101**, 944 (1956); C. Herring, E. Vogt, Phys. Rev. **105**, 1933 (1957)
8. G. Cavalleri, E. Tonni, L. Bosi, G. Spavieri, Nuovo Cim. B **116**, 1 (2001)
9. G. Cavalleri, E. Tonni, C. Bernasconi, P. Di Sia, Nuovo Cim. B **116**, 1353 (2001)
10. J.D. Jackson, *Classical Electrodynamics*, 2nd edn. (J. Wiley, New York, 1975)
11. J.R. Reitz, F.J. Milford, *Foundations of Electromagnetic Theory*, 2nd edn. (Addison-Wesley, Massachusetts, 1967), Section 15.6
12. L.G.H. Huxley, R.W. Crompton, *The Diffusion and Drift of Electrons in Gases* (Wiley, New York, 1974); for more refined expressions see G. Cavalleri, Nuovo Cim. **55**, 360 (1980); G. Cavalleri, Aust. J. Phys. **34**, 361 (1981)
13. <http://www.webelements.com>